OMNIPHOBIC LUBRICANT-INFUSED COATINGS FOR BIOSENSORS

ENHANCING BIOSENSOR PERFORMANCE WITH OMNIPHOBIC LUBRICANT-INFUSED COATINGS

By MATTHEW OSBORNE, B.Eng.

A Thesis Submitted to the School of Graduate Studies in Partial Fulfilment of the Requirements for the Degree Master of Applied Science

McMaster University MASTER OF APPLIED SCIENCE (2018) Hamilton, Ontario (Biomedical Engineering)

TITLE: Enhancing Biosensor Performance with Omniphobic Lubricant-Infused Coatings

AUTHOR: Matthew Osborne, B.Eng.

SUPERVISOR: Dr. Tohid F. Didar

NUMBER OF PAGES: xi, 63

Lay Abstract

Biosensors are an integral tool in delivering quick and accurate point-of-care diagnosis and treatment monitoring. However, their performance can be impeded by the non-specific binding of undesirable molecules and microorganisms on the sensing surface. Omniphobic lubricant-infused (OLI) coatings have been shown to suppress biofouling and blood clotting on surfaces through exceptional repellency. This thesis focuses on the implementation of OLI coatings in biosensing applications. It investigates the antibiofouling capacity of an OLI coating on a membrane for dissolved oxygen detection. Then, it discusses a novel coating with integrated DNA biosensing functionality for working directly with blood samples. The enclosed work demonstrates that the OLI coating empowers biosensors to deliver more effective point-of-care testing.

Abstract

Point-of-care testing brings diagnosis and treatment monitoring to the site of the patient. It heavily relies on biosensors, which leverage the interactions between a target biomarker and a bioreceptor, to deliver fast and accurate results. However, non-specific binding of molecules and microorganisms on the biointerface can interfere with biomarker-bioreceptor interactions and diminish a biosensor's sensitivity, specificity, and stability. In turn, this can lead to false diagnoses and ineffective treatments. Omniphobic-lubricant infused (OLI) coatings exhibit slippery, self-cleaning characteristics that repel untargeted molecules and microorganisms to augment the biosensor's performance.

In this work, we investigate the proficiency of OLI coatings in two specific applications: dissolved oxygen sensing and DNA biosensing. First, in water quality monitoring, an OLI coating is applied to the selectively permeable membranes of a dissolved oxygen sensor. Over a three-week incubation period in an environment with accelerated bacterial growth, the coated membranes exhibit a 160% higher reproducibility (10% deviation in sensitivity) and lower biofilm formation (96° static contact angle) in comparison to unmodified membranes (26%, 32°). The second application is in DNA biosensing, where a novel OLI coating uses carbon dioxide plasma activation to embed oligonucleotide probes. It demonstrates an optimized balance of slippery repellency (76° static contact angle, 10° sliding angle) and biosensing functionality, 19% longer clotting times than conventional blocking conditions, and equal sensitivity to PLL-PEG when capturing target DNA in whole blood. Going forward, our research will continue to expand the use of OLI coatings in biosensing applications, particularly exploiting its antibiofouling and anticoagulative capabilities.

Acknowledgements

I would like to thank my supervisor, Dr. Tohid F. Didar, for his remarkable guidance and support throughout my two years at McMaster University. His passion for learning and research has been formative, and I will undoubtedly use much of what I've gained from his teachings as I continue to navigate through academia and the field of biomedical engineering at large.

Second, I would like to thank Dr. Ravi Selvaganapathy, Dr. Aditya Aryasomayajula, and Dr. James Mahony for their roles in the development and success of my projects. Collaboration has been a key element of my time at McMaster University, and it has brought my education to new and exciting areas of research that have broadened my perspective on this field.

My gratitude goes to my fellow graduate students in Didar Lab, including: Maryam, Amid, Hanie, Martin, Sara, Sara, and Yuxi. They have never hesitated to offer their help or share their insight, and have set a high bar of excellence and dedication that has continuously pushed me to be a better student.

Finally, my deepest gratitude goes to Milda, my family, and my friends who have supported me relentlessly throughout my education. They have kept me grounded and optimistic, and I couldn't have enjoyed this experience as much as I did without them.

Table of Contents

List of Figures

List of Abbreviations

BSA	Bovine serum albumin
CVD	Chemical vapour deposition
DO	Dissolved oxygen
ECM	Extracellular matrix
EDC	1-ethyl-3-(3-dimethylaminopropyl) carbodiimide
eDNA	Extracellular deoxyribose nucleic acid
ELISA	Enzyme-linked immunosorbent assay
LPD	Liquid phase deposition
ncDNA	Non-complementary deoxyribose nucleic acid
NHS	N-hydroxysuccinimide
NSB	Non-specific binding
OLI	Omniphobic lubricant-infused
pDNA	Probe deoxyribose nucleic acid
PEG	Polyethylene glycol
PFOTS	Trichloro (1H,1H,2H,2H-perfluorooctyl) silane
PLL	Poly-l-lysine
POC	Point-of-care
qPCR	Quantitative (real-time) polymerase chain reaction
tDNA	Target deoxyribose nucleic acid
SAM	Self-assembled monolayer
SCA	Static contact angle
SEM	Scanning electron microscopy
ssDNA	Single-stranded deoxyribonucleic acid
UB	Unblocked
UT	Untreated
XPS	X-ray photoelectron spectroscopy

1. Introduction

The Canadian public healthcare system is one of the most expensive in the world, accounting for a predicted $242 billon, or 11.5% of the country's gross domestic product, in 2017[1]. This amounts to roughly $6600 per person yearly. Despite the high expenditures, Canadian patients must endure abnormally long wait times. With regards to this issue, the 2016 Commonwealth Fund Survey[2] places Canada's healthcare system last out of 11 countries. As part of this survey, the Canadian Institute for Health Information has reported that:

- 1 in 5 Canadians had to wait 7 or more days to see a family doctor.
- 1 in 3 Canadians had to wait 4 or more hours in a hospital emergency ward.
- 1 in 2 Canadians had to wait 4 or more weeks to see a specialist.

Going forward, these wait times will be exacerbated by an aging Baby Boomer generation. The pending increase in the senior population, who currently require 46% of healthcare expenditures despite making up only 16% of the total population[1], will lead to more patients in need of living care and greater likelihood of health complications. Furthermore, the retirement of experienced healthcare professionals will put strain on the workforce.

Canada is also known for being the country with the largest of amount of freshwater in world, totalling 20% of world's resources. However, only 35% of this freshwater is considered to be renewable, while the rest is "fossil water" that is retained in lakes, aquifers, and glaciers[3]. At face-value, this would appear to be a sufficient amount of water to serve the Canadian population (roughly 0.5% of the world's population), but excessive pollution from spills, runoff, industrial and municipal waste, and deposition of airborne pollutants has put considerable stress on the health of regional waterbodies[4]. To enact countermeasures against pollution, waterbodies must

be regularly monitored to assess the quality of their water. This can be logistically challenging and expensive considering that more than half of the country's freshwater drains into its northern regions, whereas 85% of the population lies along the southern border[3].

1.1 Point-of-Care Testing

In order to improve the cost, time, and personnel efficiencies of the healthcare system, point-of-care (POC) testing consists of a breadth of healthcare strategies aimed at bringing diagnosis and treatment monitoring to the patient's bedside. POC testing eliminates the need to send samples pulled from the patients to laboratories for conventional testing methods (*e.g.* microscopy, culture, serology, and nucleic acid amplification) that require expensive and specialized equipment, laboratory-trained professionals, and significant time requirements[5]. Patients are not required to visit testing facilities nor leave the hospital bed, which is particularly important for patients in a severely weakened state. In healthier cases, individuals can use point-of-care testing to monitor their own health at home. Commercial successes (*e.g.* pregnancy tests, urine dipsticks for bacterial infections, glucose monitors) have relied on budding handheld technologies with fast processing speeds, including cellphones, paper-based assays, and lab-on-a-chip platforms[6].

POC testing enables more patients to receive faster, more reliable, and safe diagnoses or monitoring by reducing the time spent on testing, eliminating the need for specialized technicians, and keeping the patient in a comfortable and steady position. For patients in critical care, this can be crucial in delivering the appropriate and effective treatments needed to save lives. POC testing's lower costs also eases financial expenditures on the public healthcare system by the federal government. The saved funds could be reinvested in other areas of the healthcare

system: infrastructure, disease prevention and treatment, health education, or palliative care to name a few.

1.2 Water Quality Testing

In remote locations, integrated and cost-effective testing strategies need to be employed to monitor water quality levels. First, it is expensive and time-consuming to have highly specialized environmental scientists travelling across the country to individually analyze regions. Instead, a device that generates fast readings and operates simply empowers local populations to monitor their own water bodies. It is also ineffective to bring samples from remote locations to centralized laboratories since the properties of samples are likely to change during transport, particularly if it has high microbial growth. Thus far, a variety of properties and analytes have been monitored to evaluate water quality, including: pH, turbidity, conductivity, temperature, salinity, phosphate, nitrate, chlorophyll, and dissolved oxygen[7–9]. Hence, there is a growing need for point-of-source sensing technologies not only in the field of medicine but also in environmental sciences.

1.3 Biosensors

To provide effective POC and water quality testing, engineers and technologists need to downsize equipment, reduce response times, and lessen workforce specialization by designing with integration and simplicity of use in mind. Biosensors aim to integrate the diagnosis and/or monitoring processes into a single analytical device. The target analyte(s) of a biosensor are typically whole cells or biological molecules (biomolecules), which are further classified into: proteins, carbohydrates, lipids, nucleic acids, and metabolites. An analyte is considered a biomarker if either its mere presence or a fluctuation in its concentration level corresponds to the onset or progression of a disease[10].

Biosensors can interact with a biomarker using a bioreceptor: a different biomolecule or cell with a biochemical affinity to the target biomarker. The bioreceptor is immobilized on a solid substrate so that the capture event separates the analyte from the working sample. The surface is then considered to be biofunctional. The working sample originates from the patient and is most often an easily-accessible fluid such as blood, urine, saliva, sweat, or semen[11]. The region consisting of the substrate's surface, the immobilized bioreceptors, and the interacting portion of the working sample is called the biointerface (**figure 1.1**). Bioreceptor immobilization can be achieved either physically (physisorption) or chemically (chemisorption). Physisorption relies on Van der Waals and hydrophobic interactions, which are simpler to manage procedurally but are at risk of producing multiple layers and leaching into the working sample[12]. Also, in the absence of electrostatic polarity, the bioreceptors may adsorb in ineffective orientations where the bioreceptor is oriented towards the substrate instead of the working sample[13]. Chemisorption, on the other hand, involves covalent bonding between the bioreceptor and the substrate. It provides higher bond energy for superior physicochemical stability[14], facilitates the fabrication of monolayers, and can ensure specific orientation[15].

After the biointerface is incubated with the working sample for a time duration suitable for biomarker-bioreceptor coupling, the sample is removed and a transducer is used to detect the captured biomarkers. Upon detection, the transducer produces a signal proportional to the quantity of captured biomarkers, which can then be read directly by the user or fed to a processor. A processor is employed to convert the signal into a more readily-analyzable format (*e.g.* digital). Additionally, it may integrate any necessary mathematical analysis into the biosensor so that the output is directly indicative of the disease's presence or progression.

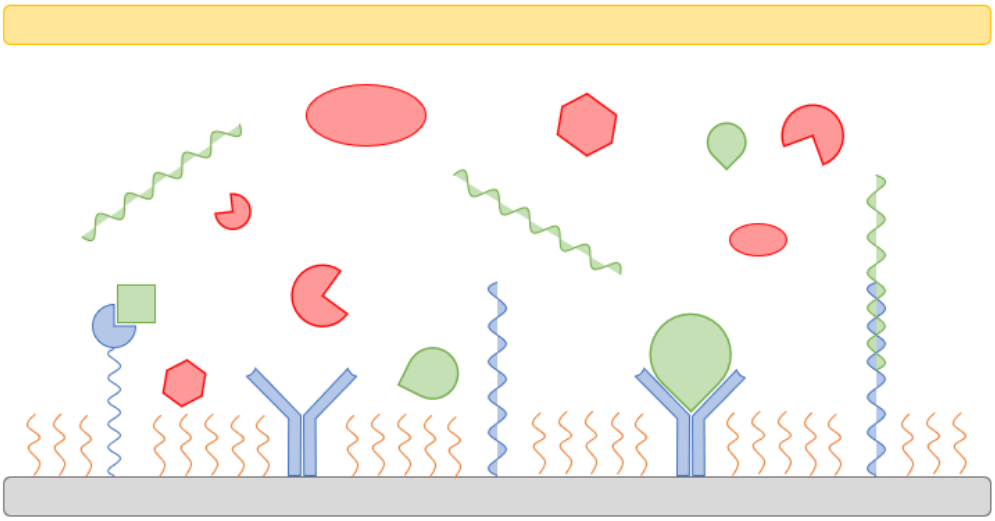

Figure 1.1. Composition of the biosensor. Bioreceptors (blue) are immobilized on a solid substrate (grey) and bind to biomarkers (green) in the working sample. A transducer (yellow) detects bioreceptor-biomarker binding and produces a proportional signal. Surface blockers (orange) prevent non-specific binding of biomarkers and untargeted molecules (red) to the substrate.

1.3.1 Design Parameters

When designing a biosensor, there are numerous parameters that need to be considered, and an optimal balance of these parameters must be established for clinical or commercial relevance. These parameters can be performance-related, meaning that they can directly impact the biosensor's output. Otherwise, practical parameters can influence how the biosensor is implemented in a clinical or commercial setting.

The principal performance parameter of biosensors is sensitivity, which is defined as the signal output over input. In this context, a high sensitivity refers to a large change in the transducer's output signal as a response to a small increase in biomarker capture. A high sensitivity typically corresponds with a high resolution, which is the biosensor's capability in

discerning a minimal increment in biomarker capture, and high range, which describes the minimum and maximum biomarker concentrations that it can detect. With a low sensitivity, a biosensor would not be capable of properly quantifying the change in a biomarker's concentration, which can be crucial for disease staging[16]. Alternatively, at lower biomarker concentrations, it may fail to detect its presence at all and deliver a false negative diagnosis. In this case, an unknowingly-diseased individual would be medically cleared, but the disease would continue to progress untreated until new symptoms arise.

Specificity describes the biointerface's effectiveness at exclusively interacting with target biomarkers. Hence, a biosensor whose output can fluctuate as a result of nontargeted molecules or operating conditions is considered to lack specificity. This is a common consequence of non-specific binding (NSB), where nontargeted molecules adhere to unoccupied areas of the biointerface via physisorption. Despite not interacting with the bioreceptor, some transducers may interpret NSB as successful target capture. Alternatively, a poorly-selected bioreceptor may interact with other components of the working sample, rather than just the target biomarker. Even in the case where the transducer doesn't report these non-specific interactions, the bioreceptors are no longer available to capture biomarkers, thus reducing the sensitivity. The transducer may also exhibit undesirable signal fluctuations or "noise" as a result of immediate environmental factors (*e.g.* external magnetic fields, temperature, vibrations, etc.)[17]. Low specificity can lead to a false negative or false positive diagnosis. With false positive diagnoses, sick patients are treated for the wrong disease; hence, treatment would be ineffective and the disease would progress. For healthy patients, a false diagnosis would lead to the treatment of a condition despite not having one, resulting in unnecessary costs and potential side-effects.

Stability refers to the biosensor's ability to deliver accurate results over time and in different conditions. A poor stability can be the result of bioreceptor degradation in a manner that causes desorption or prevents it from interacting with the biomarker. Bioreceptors can potentially degrade with time or under variations in temperature or salinity[18]. Otherwise, transducer degradation can also prevent it from recognizing bioreceptor-biomarker interactions (*e.g.* photobleaching of fluorescent dyes)[19]. Even if it is properly managed, a biosensor with a short shelf-life results in excessive waste. On the other hand, if a biosensor with a long shelf-life is unproperly stored or used, the sensitivity or specificity of the biosensor are at risk of being compromised.

To deliver reliable results, biosensors must have high reproducibility, meaning that it produces identical readings under duplicated operating conditions. A low selectivity and stability can cause significant and indeterminate deviations (*i.e.* inaccuracy) in readings that would render the biosensor clinically irrelevant.

Considering the time-sensitive nature of diagnostics, it is important that biosensors are able to deliver an analysis as quickly as possible. With quickly progressing diseases, doctors may have only a few hours to make a diagnosis and develop a treatment strategy. Due to the near instantaneous interactions between most bioreceptors and biomarkers, biosensors should have response times that only require minutes to an hour to execute. Culturing methods, on the other hand, can take days and still result in false diagnoses.

Finally, it is important to consider the many parameters that may prevent a strong engineering design from being used in practical applications. The cost of a biosensor must be minimized by selecting efficient materials and emphasizing low consumption. If the biosensor is significantly more expensive than comparable conventional methods, it will not gain much

traction in a publicly-funded healthcare system. Device reusability helps reduce capital expenditures and the environmental impact. The biosensor must be physically robust; persistent damage and maintenance increases the need for professional repair and its associated costs. It also puts the biosensor at risk of delivering false results if the damage goes undetected. Through the complete integration of the biointerface, transducer, and processor, the biosensor should be simple to operate and to obtain readings from. If not, this could jeopardize the safety of both the operator and the patient. Furthermore, the inclusion of hazardous materials or by-products in the biosensor's design should be avoided; if necessary, these substances should be well contained.

1.3.2 Types of Bioreceptors

Selecting an optimal bioreceptor for a given biomarker is the first step in designing the composition of a biosensor. Although research has been done on fabricating synthetic bioreceptors for biomarkers, the most common and effective pairings are those found in nature[20].

Antibodies are y-shaped proteins produced by the immune system to recognize and bind with specific molecules on pathogens, which can either disable the pathogen or tag it for destruction by macrophages. These specific molecules are referred to as antigens, and make up a significant portion of disease biomarkers. The antigen binds to a site at the end of either "arm" of the antibody in a lock-and-key manner, referring to its high specificity[21]. Therefore, antibodies are useful bioreceptors for conventional pathogenic diseases. However, the antibody-antigen binding is generally irreversible and strongly dependent on physiochemical assay conditions[22].

Enzymes are catalytic proteins, meaning that they undergo a biochemical reaction when interacting with an analyte. For biosensors, this allows a transducer to either measure the activation of the enzyme or a direct product of the biochemical reaction. Enzymes are not consumed during the reaction, and can therefore be used for multiple detections[22]. They have

been used for a variety of analytes (*e.g.* products, substrates, inhibitors), but are considered to be less stable than other bioreceptors[22].

Nucleic acids include ribonucleic acids (RNA) and deoxyribonucleic acids (DNA). Both the bioreceptor and the biomarker are single strands of RNA or DNA, and highly specific biorecognition occurs through complementary base pairing[23]. The role of nucleic acids as bioreceptors, including synthetic variations such as aptamers and DNAzymes, is reported in further detail in chapter 3.

Aside from biomolecules, organelles and whole cells can be attached to surfaces and act as bioreceptors. Whole cells are capable of responding to a variety of biological, chemical, or mechanical stimulants. They can produce a variety of enzymes in response to such stimulants and reveal evidence of toxicity[24]. Individual organelles can likewise produce their own enzymes in response to biomarkers. The organelles and cells must be strictly maintained at their respective biological conditions, and are prone to shorter shelf-lives.

1.3.3 Types of Transducers

The role of the transducer is to detect the presence of biomarker-bioreceptor interactions and to proportionally relate these interactions to a quantifiable signal. Biosensor transducers can be categorized as optical, electrochemical, gravimetric or thermal.

Optical transducers transmit light in response to biomarker capture. In fluorescence tagging, reporter molecules, each containing a fluorophore, are introduced to the biointerface and interact specifically with the immobilized biomarkers. Their presence can then be relatively quantified from the fluorescence intensity observed using an integrated imaging system or external apparatus such as a fluorescence microscope. Colorimetric and chemiluminescent

molecules can also be used instead of fluorescence[25]. They are easy to visualize with the naked eye and provide fast readings, but they are not as simple to quantify and are typically single-use. When considering reporter molecules, a blocking agent is essential; otherwise, NSB of reporter molecules will artificially increase the biosensor's signal. The miniaturization of conventional optical laboratory instruments has enabled their integration into biosensors. Surface plasmon resonance measures the increase in refractive index of the biointerface with biomarker capture, and has been implemented in the development of a portable biosensing system[26], but this technique again fails to account for the differentiation between specific and non-specific interactions on the biointerface . Progress has also been made in miniaturizing real-time polymerase chain reaction (qPCR), but have not yet approached the high sensitivities of benchtop qPCR instruments[27].

Electrochemical transducers are capable of directly producing an electrical signal proportional to the presence of chemical reactions between the bioreceptors and biomarkers. A common technique is to use a gold-plated substrate and immobilize thiol-terminated bioreceptors; the thiol group bonds covalently with the gold surface[28]. As biomarkers bind with the bioreceptors, the impedance of the biointerface increases[29], and this can be observed by a decrease in current through the gold layer at a constant voltage. NSB can tamper with the impedance measurements, resulting in signal noise that lowers the measurement accuracy[30]. Similar to fluorescent tagging, magnetic nanoparticles have been used to label captured biomarkers[31]. Electrochemical biosensors demonstrate high levels of integration and potential for miniaturization[24], which makes them a preferred approach in point-of-care testing.

Gravimetric transducers are force-sensitive piezoelectric materials that are typically implemented in the form of quartz crystal microbalances or microcantilever beams. Quartz

crystal microbalances contain quartz-electrode sandwiches with immobilized bioreceptors[32]. Biomarker capture alters the resonant frequency of quartz and produces a fluctuation in the electric field. Similarly, microcantilever beams use piezoelectric crystals that undergo elastic deformation from changes in mass and produce electrical signals as a result of bioreceptor-biomarker binding[33]. Considering the size of the biomarkers, the structures in gravimetric transducers must be very small; hence, advanced microfabrication methods are required. Again, these transducers are susceptible to loss in specificity as a result of mass change due to NSB.

Thermometric transducers are implemented with enzyme bioreceptors that yield changes in temperature as a product of a biochemical reaction. The change in temperature can be perceived by a pyroelectric material that produces an electrical signal without the need for a power source[34]. However, these transducers are not pertinent to bioreceptor-biomarker interactions that produce little to no temperature change.

1.3.4 Surface Blocking Strategies

As previously discussed, a biosensor's specificity can be critically diminished by the NSB of untargeted molecules or microorganisms on the biointerface. Additionally, NSB of larger entities can sterically hinder or completely block bioreceptors from interacting with biomarkers, thus reducing their sensitivity as well. To minimize NSB, surface blocking agents must be added to the biointerface to cover any surface area that is not occupied by a bioreceptor. These blocking agents must be chemically inert, especially with the chosen biomarker and bioreceptor. Smaller blocking agents are advantageous in avoiding steric interactions with bioreceptors. Similar to bioreceptors, blocking agents can be immobilized on the surface using physisorption or chemisorption. Since a blocking agent is typically added to the biointerface after the bioreceptor

is immobilized, most strategies use physisorption so that the blocking agent does not need to rely on surface functional groups for covalent binding.

Conventional blocking agents usually fall into one of three groups: proteins, polymers, and surfactants. Bovine serum albumin (BSA) is a protein with a well-established history of surface blocking in immunoassays, such as Western blots and enzyme-linked immunosorbent assays (ELISAs)[35–37]. Compared to other proteins, it has low reactivity, small size, and high stability, but these properties are lesser than other non-protein blocking agents[38]. BSA also generates air bubbles that can be disadvantageous in biosensors with microchannels. Protein mixtures such as non-fat dry milk and gelatin are readily-available and cost-effective alternatives[39]. These mixtures are heterogeneous and do not coat the surface evenly, which could cause certain areas of the biointerface to be at a higher risk of NSB over others.

There are numerous polymers that are capable of acting as a blocking agent. In particular, polyethylene glycol (PEG) has become a gold standard for surface blocking[40]. It exhibits very low reactivity and its size can be tuned during synthesis. Polymers do not undergo denaturation like proteins, and are therefore significantly more stable at higher temperatures and acidic conditions. By itself, though, PEG adsorption is not very effective. Instead, it is often grafted to other polymers, namely poly-l-lysine (PLL) and polyethyleneimine, that have a strong electrostatic affinity to charged surfaces[41,42]. Other polymers that have been used for surface blocking include polyacrylamide[43], polyallylamine hydrochloride[44], polystyrene sulfonate[44], polyvinylpyrrolidone[45], and polyvinylsulfonic acid[44], but these have not been evaluated nearly as extensively for surface blocking as PEG.

Surfactants are compounds known for increasing surface wettability and acting as a detergent, but can also be used as blocking agents in low concentrations and in conjunction with

other blocking agents[46]. Tween 20 (which contains 20 repeat units of PEG)[37], sodium dodecyl sulfate[44], cetrimonium bromide[44], and Triton X-100[45] are examples of surfactants that have been used for surface blocking. However, their cellular toxicity, tendency to denature proteins, and substantial bubbling make them a less favourable option for biosensors[47].

1.4 Omniphobic Lubricant-Infused Coatings

There is an emerging surface blocking strategy that can be collectively referred to as omniphobic lubricant-infused (OLI) coatings[48–51]. This strategy was inspired by the carnivorous *Nepenthes* pitcher plant[52]. When dry, insects are able to move freely along its surface with ease. However, after rainfall, micro-structuring on the peristome, the lip at the top of the pitcher, is capable of capturing a thin layer of water[53]. As insects move onto this region of the plant, they are unable to properly adhere, causing them to slip and fall into the pitcher for digestion. OLI coatings similarly consist of a thin lubricant layer that is held by a physical and/or chemical affinity against a substrate's surface[54]. This lubricant layer gives the surface a high degree of slipperiness and repellency. As such, the coating is considered to be self-cleaning.

The affinity between the lubricant layer and the substrate can be achieved through one or a combination of two approaches. Nano- or micro-structuring of the substrate involves inducing or adding geometrical features in a repeated pattern to induce a porous texture along the surface. These features have included nanopillars[55–57], wrinkling[58,59], and honeycombs[60]. The other approach is to immobilize molecules on the surface in self-assembled monolayers (SAMs) that have an intrinsic affinity to the composition of the lubricant. Badv *et al*. used a silane SAM with long fluorocarbon chains to capture a thin layer of highly fluorinated lubricant, perfluorodecalin[61]. Considering the hydrophobic and oleophobic nature of fluorine, this coating

provides an "omniphobicity" that exhibits a high repellency to an extensive variety of aqueous and organic fluids, as well as solid particles.

Since it was first developed by the Aizenberg group at Harvard University in 2011[54], the self-cleaning properties of OLI coatings have shown to be serviceable in numerous areas of research. It has been studied for airplane wings and ship hauls to prevent ice buildup at high altitudes and frigid waters[62,63]. The proficiency of OLI coatings in inhibiting biofouling has also extending its application to marine[64] and water treatment infrastructure. In the broader spectrum of micro total analysis systems, slippery surfaces reduce friction along microfluidic channels, thus resulting in a low friction interface and smoother flow or droplet manipulation[65]. In medical technologies, OLI coatings have been proven to avert thrombosis[66], meaning that it attenuates blood clotting resulting from the contact between blood and the biointerface (*i.e.* contact/intrinsic pathway). Catheters have been successfully coated with the aim of improving biocompatibility by reducing thrombotic complications when inserted *in vivo*[61].The antibiofouling and anticoagulative nature of OLI coatings will be investigated further in chapter 2 and 3, respectively.

1.5 Thesis Objectives

The overarching objective of this thesis is to investigate the implementation of OLI coatings in biosensing applications. Its self-cleaning properties were paired with biosensing functionality to address coagulation and biofouling in practical circumstances. The detailed objectives for the two projects discussed in this thesis are as follows:

- Demonstrate that an OLI coating on the selectively permeable membrane for a commercial dissolved oxygen sensor diminishes the rate of biofilm formation in a heavily bacteria-concentrated environment (chapter 2).
- Evaluate how the coated membrane impacts the sensor's stability with increased time undergoing biofouling in comparison to an unmodified membrane (chapter 2).
- Design a novel biofunctional OLI coating with integrated oligonucleotide probes for DNA biosensing (chapter 3).
- Demonstrate that the designed coating attenuates the rate of blood coagulation more effectively than conventional blocking agents (chapter 3).
- Demonstrate that the designed coating enables the capture of target DNA in whole blood solutions with higher sensitivity and selectivity than conventional blocking agents (chapter 3).

2. Suppression of Biofouling on a Selectively Permeable Membrane for Dissolved Oxygen Sensing using an Omniphobic Lubricant-Infused Coating

Matthew Osborne [a], Tohid F. Didar [a,b,c], P. Ravi Selvaganapathy [a,b], Aditya Aryasomayajula [b], Amid Shakeri [b]

[a] School of Biomedical Engineering, McMaster University, Hamilton, Ontario, Canada

[b] Department of Mechanical Engineering, McMaster University, Hamilton, Ontario, Canada, Canada

[c] Institute for Infectious Disease Research (IIDR), McMaster University, Hamilton, Ontario, Canada

Author Contributions: MO was involved in the design and execution of all experiments and data analysis. TD was involved in the experimental design, supervised the project to completion, and provided financial support. RS contributed to the experimental design, and provided both valuable insight and financial support. AA was involved in the preliminary planning of the project. AS conducted the SEM imaging with MO. MO wrote the manuscript with contributions from TD.

2.1 Abstract

A tolerable concentration of dissolved oxygen (DO) must be maintained in a waterbody for it to be hospitable for aquatic animals. DO sensor designs can employ selectively permeable membranes to isolate DO from untargeted compounds or organisms in waterbodies. Hence, the DO concentration can be monitored and the health of the water evaluated over time. However, the presence of bacteria in natural waterbodies can lead to the formation of biofilms that can block pores and prevent analyte from permeating the membrane, resulting in inaccurate readings.

In this work, we investigate how the implementation of a fluorosilane-based omniphobic lubricant-infused (OLI) coating affects the rate of biofilm formation on a selectively permeable membrane for a commercially-available DO sensor. Coated and unmodified membranes are incubated in an environment undergoing accelerated bacterial growth, and the change in sensitivity is evaluated after periods of 40, 100, 250, and 500 hours. Our findings show that the OLI membranes successfully maintain an accurate sensitivity (10.3% deviation from non-biofouled control) after three weeks in comparison to unmodified membranes (26.0% deviation). Fluorescence and scanning electron microscopy of biofouled membranes depict a significantly reduced rate of biofilm formation on the OLI coating. The decrease in static contact angle is more significant on unmodified membranes (113.9° to 32.1°) than on coated membranes (119.4° to 96.3°) after three weeks.

Keywords: biofouling; bacteria; biofilm; membrane; omniphobic; lubricant-infused; coating; dissolved oxygen.

2.2 Introduction

Natural waterbodies are a critical part of our biosphere and are predicted to be the home to a half-million different eukaryotic species[67]. These species rely on oxygen intake from dissolved oxygen (DO) gas, and fluctuations in DO concentration levels can be fatal. Diverse fish populations typically require between 7 mg/L and 10 mg/L to thrive. However, excessive pollution can result in hypoxic water conditions with concentrations below 4 mg/L[68,69]. Handheld DO meters present a reliable and convenient method to monitor the DO concentration in waterbodies and identify whether aquatic species are at risk of hypoxia. In this work, we consider the ExStik II DO meter from Extech Instruments. This electrochemical DO sensor employs a cap-bound selectively permeable membrane with an electrode immersed in

electrolytic solution. DO is the sole compound capable of diffusing through the membrane, after which it alters the conductivity of the electrolytic solution. By isolating DO from other compounds, the selectively permeable membrane reduces background noise, leading to higher accuracy and reading stability.

In marine environments, planktonic bacteria are capable of detecting and adhering to solid surfaces via electrostatic interactions[70], subsequently initiating biofilm formation (**figure 2.1a**). Multi-species groups of bacteria physically adhere in clusters on the surface and subsequently produce a viscous extracellular matrix (ECM) containing polysaccharides, proteins, phospholipids, and extracellular DNA (eDNA)[71]. Reproduction continues as the microcolony matures into a mushroom-shaped biofilm. Bacteria in the bottom layers downregulate their flagella and enter a state of sessile growth.[72] Finally, newly-produced planktonic bacteria are ejected from the biofilm to form new biofilms elsewhere in the environment.

While selectively permeable membranes are an advantageous component in sensor design, they can provide a suitable surface for bacteria adherence. In the case of polluted waters, where DO concentrations are lower than needed for aquatic animals but advantageous for anaerobic bacterial growth, the membranes are at particular risk of provoking biofouling. When this occurs, a biofilm is capable of blocking pores and prevent the target molecules from diffusing through the membrane, rendering the sensor inaccurate or perhaps inoperable. Furthermore, bacterial ECM are known to consist of acidic compounds that corrode submerged surfaces[73].

To discourage biofilm formation, surfaces can be coated with blocking agents that inhibit the physical attachment of bacteria. Marine antibiofouling is a longstanding area of interest in scientific and military research due to the corrosive and drag-increasing effects of biofilms on

submerged vessels and infrastructure. A number of metallic (*e.g.* copper, silver) and biocidal nanoparticle coatings have been achieved[74–76], but such cytotoxic chemicals can leach into waterbodies and result in adverse environmental effects[77]. The food and beverage industry has also employed antibiofouling coatings to limit spoilage and pathogen transfer between items[78]. These coatings are organic in nature and must be safely digestible in the case of direct contact with food. Similarly, the healthcare and dentistry industries use surface blocking strategies to prevent infections during implantation[79,80]. Common examples of organic blocking agents for biofouling include inert proteins, organosilanes[73], and polyethylene glycol[81,82].

Alternatively, there is an emerging class of antibiofouling surface blocking agents called omniphobic lubricant-infused (OLI) coatings. They rely on the capillary forces induced by micro/nano-scale texturing or chemical affinities to lock a thin layer of lubricant over the treated surface[55,83]. When a foreign liquid is introduced to the surface, the resulting liquid-lubricant interface offers a high degree of repellency and "slipperiness" that prevents adhesion of the liquid as well as any entities suspended in it[84]. Ware *et al.* has investigated the use of a lubricant-infused nano-wrinkled polymeric surfaces in marine environments and has shown that its antibiofouling properties are effective on nonporous surfaces[83]. However, nano-wrinkling poses complications in fabrication and membrane permeability that are better addressed by a tethered liquid perfluorocarbon approach first demonstrated by Leslie *et al.* [85]. Badv *et al.* used a highly fluorinated lubricant (perfluorodecalin) with a high affinity to a silane self-assembled monolayer (SAM) containing long perfluorocarbon functional chains produced using chemical vapor deposition[61].

In this study, we investigate the application of an antiadhesive fluorosilane-based OLI coating to the selectively permeable membrane of the ExStik II DO meter (**figures 2.1b-d**). By

accelerating bacterial growth in tap water using yeast extract[86], untreated (UT) and OLI membranes were incubated in a highly concentrated bacterial environment for up to three weeks. After set time intervals, biofilm formation was observed and characterized using sensitivity readings, fluorescence microscopy, scanning electron microscopy (SEM), and static contact angle (SCA) measurements. We hypothesized that the OLI coating prevents bacterial adhesion more effectively than UT membranes yet allows DO to diffuse through unhindered. This would lead to a more stable sensitivity over time and accurate measurements of DO concentrations.

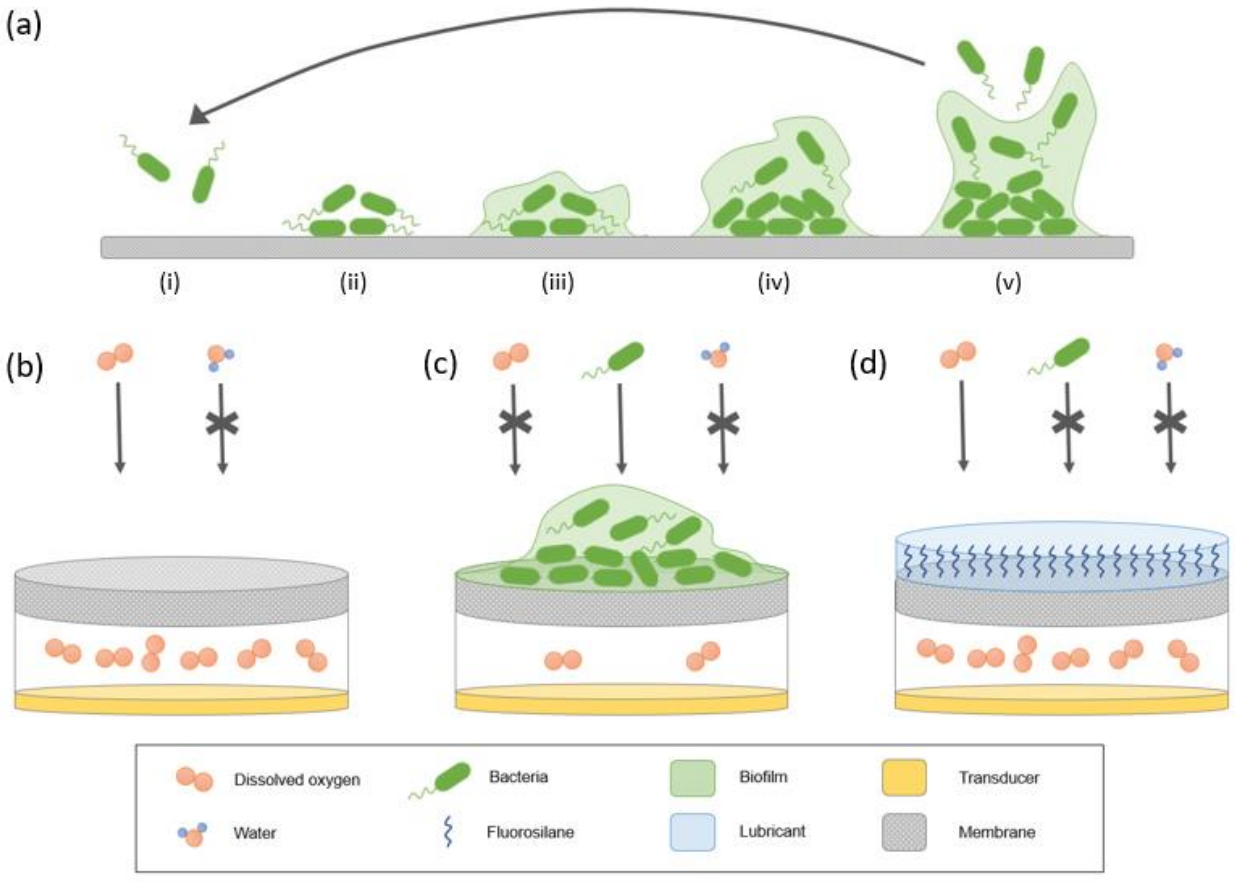

Figure 2.1. Schematic of biofouling on untreated and treated membranes. (a) Progression of biofilm formation, including (i) detection of submerged surface, (ii) bacterial adsorption, (iii)

ECM excretion, (iv) mature biofilm, and (v) ejection of planktonic bacteria. (b) In clean water, the selectively permeable membrane allows DO to diffuse through but repels water and large compounds. (c) Practically, the bacteria living in natural waterbodies adhere to the membrane's surface over time. They form biofilms that limit particles, including DO, from passing through the membrane. (d) The fluorosilane-based OLI coating prevents bacterial adhesion and ensuing biofilm formation but allows dissolved oxygen to diffuse through both the coating and the membrane.

2.3 Methods

Materials. The ExStik II DO600 dissolved oxygen meter and DO603 membrane kits were purchased from Extech Instruments (Nashua, USA). Powdered yeast extract was purchased from BioShop (Burlington, Canada). Trichloro (1H,1H,2H,2H-perfluorooctyl) silane (PFOTS), 4′,6-Diamidino-2-phenylindole dihydrochloride (DAPI), and perfluorodecalin was purchased from Sigma-Aldrich (Oakville, Canada). Phosphate buffered saline (PBS) was prepared in-house. Formaldehyde was purchased from Caledon Laboratories (Georgetown, Canada).

Oxygen plasma activation. Oxygen plasma was used to induce hydroxyl groups on membrane surfaces for covalent attachment of PFOTS. Selected membranes were oxidized using medical grade oxygen gas and a Herrick PDC-001 (115V) plasma cleaner for 2 minutes at 450 mTorr.

Liquid phase deposition (LPD). Immediately after plasma activation, the membranes were partially submerged in a solution containing 5% PFOTS in ethanol by volume so that only the exterior surface of the membrane was in contact with the solution. The membranes were incubated for 2 hours so that the PFOTS arranges itself in a SAM[87]. Subsequently, they were baked on a hot plate at 60°C for a minimum of 6 hours to promote the formation of covalent

bonds and evaporate hydrochloric acid, a by-product of the reaction. Samples were then sonicated in ethanol for 20 minutes to remove any unbound PFOTS.

Accelerated bacterial growth environment with yeast extract. An environment that stimulates accelerated multi-bacterial growth was prepared in a glass dish using 1 g yeast extract and 100 mL tap water. OLI membranes were first saturated in perfluorodecalin for 30 seconds, then all membranes were partially submerged in the yeast solution. The container was mostly covered, but air was allowed to pass in to re-oxidize the solution and avoid mass bacterial death. Membranes (3 OLI and 3 UT) were removed and tested at 40, 100, 250, and 500 hours.

Sensitivity readings. The biofilms were fixed with 4% formaldehyde in 1X PBS for 30 minutes. The DO meter equipped with UT or OLI membranes were used to take readings in tap water at roughly DO concentrations of 4 mg/L, 3 mg/L, 2 mg/L, and 1 mg/L. Tap water was recorded at 4 mg/L, and the subsequent concentrations were achieved by bubbling nitrogen gas in the tap water for 7 seconds, 15 seconds, and 30 seconds respectively. The exact concentrations were verified using a non-biofouled or "clean" UT membrane. The readings were plotted against those given by the clean membrane and fitted with linear trendlines, and the slopes were compared over time.

Fluorescence microscopy. Biofouled membranes were stained with 200 µL of 71.5 µM DAPI in 1X PBS for 1 hour and rinsed lightly with distilled water for 5 seconds. Images were taken with a Zeiss AX10 inverted microscope with ApoTome.2 fluorescence functionality. Fluorescence intensity was quantified using ImageJ image processing software. The 2 highest and lowest values were removed for each condition.

Static contact angle measurements. SCA measurements were taken using a Future Digital Scientific Corporation OCA 35 contact angle meter on the air-dried membranes with 1 µL sessile droplets of deionized water.

Scanning electron microscopy. Biofouled membranes were cut from their caps and coated in a 36 nm layer of gold. SEM images were obtained using a Tescan VEGA II LSU at 10 kV and 5000x magnification.

Statistical analysis. Data are presented as means ± S.D. Statistical significance was assessed using analysis of variance and post-hoc analysis with Tukey's test, where significant difference was considered as $P < 0.05$.

2.4 Results

A total of 12 membranes were coated using LPD with a 5% PFOTS solution as described in the methods. These OLI membranes and 12 UT membranes were used to take calibration readings at DO concentrations of roughly 4 mg/L, 3 mg/L, 2 mg/L and 1mg/L. The readings were plotted in three sets of eight (4 UT and 4 OLI) against a corresponding set of UT readings in **figure 2.2**, and then fitted with linear trendlines. In the case where UT values were plotted against themselves, the linear trendlines had a unitary slope and overlaid one another. The OLI trendlines, on the other hand, demonstrated a slight average deviation in slope of 2.3% ± 0.9%.

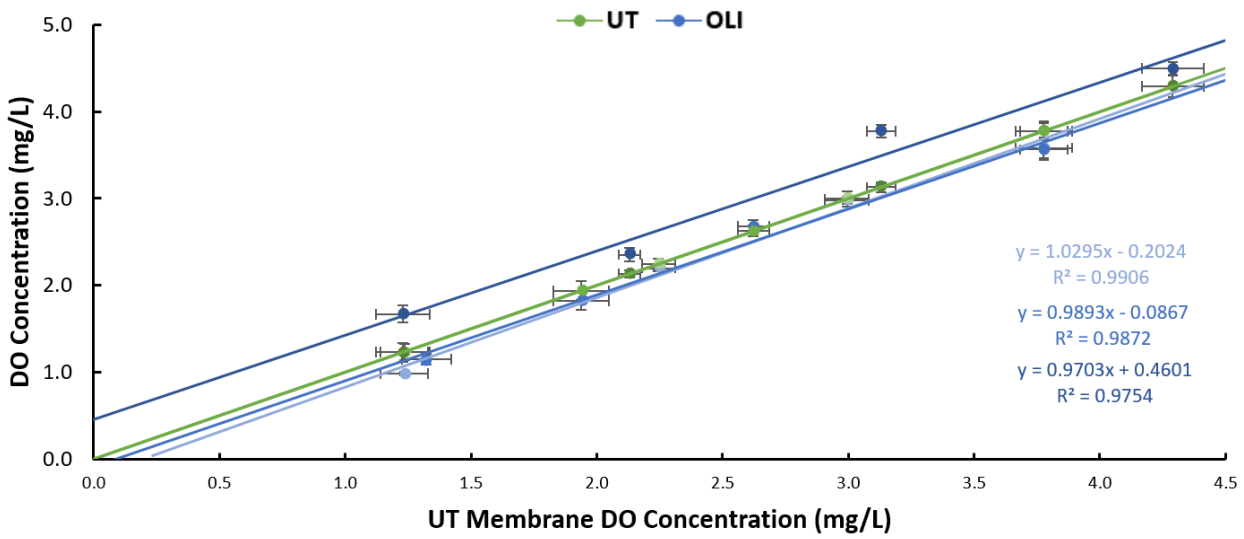

Figure 2.2. Calibration of DO sensor with UT and OLI membranes before biofouling. UT membranes are plotted against themselves, resulting in a single trendline with a unitary slope (green). Each set of OLI membranes (shades of blue) show a minor deviation in slope.

Incubation took place in a concentrated bacterial environment for varying time periods (40 hours, 100 hours, 250 hours, and 500 hours). At each interval, sets of 3 OLI and 3 UT samples were removed and readings were taken as described in the calibration. **Figure 2.3** shows how the slope of each plotted trendline, which delineates the sensitivity, changes with each set of membranes as an absolute percentage. The values obtained using the biofouled membranes were plotted against those taken using an untreated and non-biofouled membrane. The UT curve slopes upwards at a consistent rate, peaking at a deviation of 26.0% ± 1.1%. The OLI curve shows relatively little change between 40 hours and 500 hours, generally falling between 4-9%. As a result, after at least 80 hours of biofouling, the DO sensor equipped with OLI membranes consistently produced more accurate readings than the UT membranes.

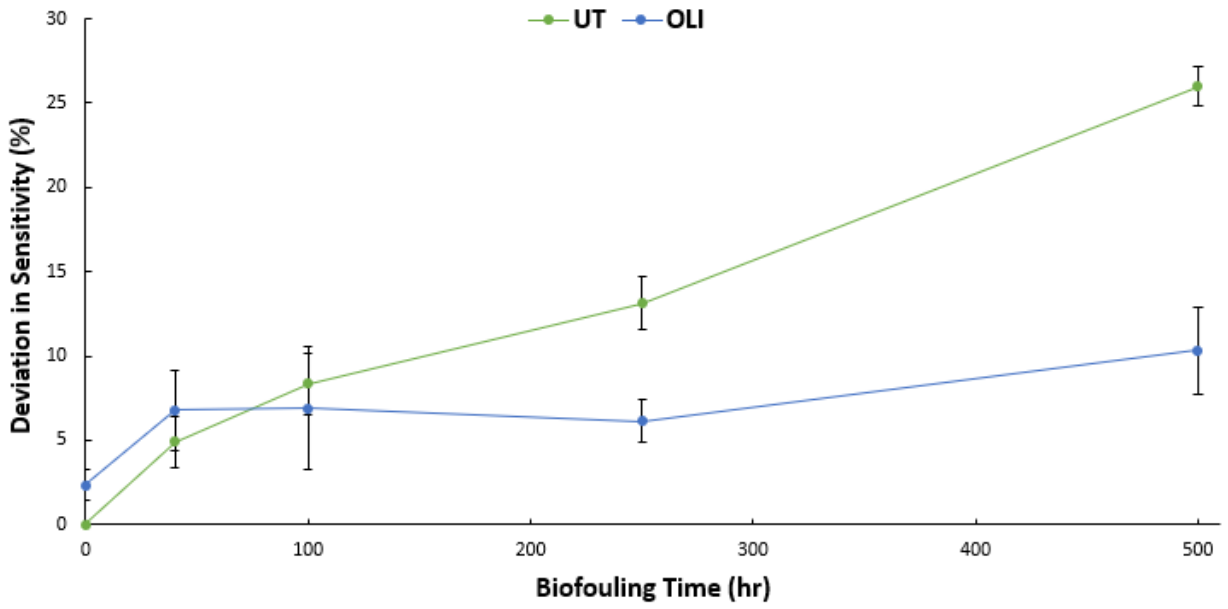

Figure 2.3. Variation in sensitivity of DO sensor with increasing time that membranes spend biofouling. UT membranes demonstrate a sharper deviation in sensitivity than OLI membranes over a 3-week period. The two conditions are equal after approximately 3 days, but UT membranes have a 160% higher deviation than OLI membranes by the end of the 21-day experiment.

All membranes were stained with DAPI, a blue fluorophore that binds to the A-T nucleotides on both the DNA inside the fixed bacteria as well as eDNA in the ECM. Fluorescence microscopy was subsequently used to characterize the biofilm distribution (**figures 2.4a-b**). Immature biofilms at the 40-hour mark featured dimmer blue regions of sparser individual bacteria and eDNA, and bright blue clusters of denser bacterial microcolonies. As the density of the biofilms increased with time, the images correspondingly increased in brightness and homogeneity. After 21 days, UT membranes featured dense and uniform biofilms over the entirety of the surface. On the other hand, biofilms on OLI membranes were notably dimmer and had various amorphous areas with little to no growth.

Figures 2.4c-d are SEM images of membranes after 21 days of biofouling at 5000x magnification. The biofilm distribution on the UT membranes is significantly denser and more homogeneous in comparison to the OLI membranes, which agrees with the fluorescence analysis. Accordingly, the OLI membranes exhibit more unhindered surface area for gas permeation.

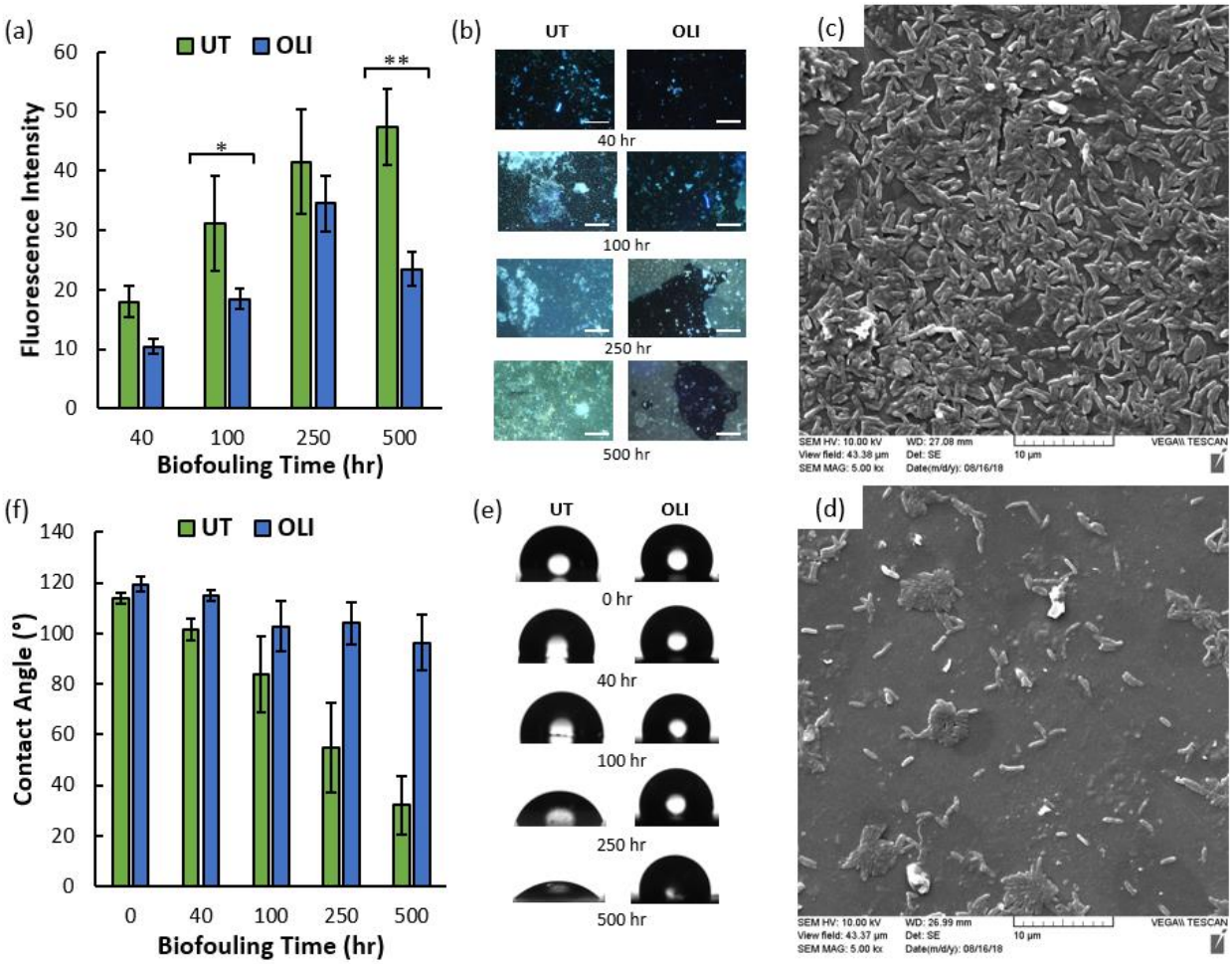

Figure 2.4. Characterization of biofilm density and distribution on biofouled membranes. (a, b) Both UT and OLI membranes show an increase in fluorescence intensity with time. The untreated membranes increase in fluorescence intensity at a higher rate and its biofilm distribution is more homogeneous. Scale bar = 200 µm. *, **Significant difference in fluorescent

intensity between the UT and OLI samples ($P < 0.05$). (c) SEM images of UT membranes after 21 days depict a thick and homogeneous biofilm. Scale bar = 10 µm. (d) Meanwhile, isolated bacterial clusters and individual bacterial are sparsely distributed on the OLI membranes after 21 days. (e, f) UT membranes, initially hydrophobic (113.9° ± 2.1°), become more hydrophilic as biofouling progresses. After 21 days, biofilm formation leads to very hydrophilic conditions (32.1° ± 11.7°). OLI membranes (initially 119.4° ± 2.9°) maintain hydrophobicity over the 3-week period with only a 21.3° decrease in contact angle.

SCA measurements quantify the surface energy and repellency of the membrane surface (**figures 2.4e-f**). Surfaces with an angle over 90° are considered to hydrophobic, whereas those under are hydrophilic. Out of the package, the UT membranes are hydrophobic with a SCA of 113.9° ± 2.1°. This is critical to the design of this selectively permeable membranes since it relies on hydrophobicity to enable gas mass transfer while rebuffing water molecules[88]. The OLI treatment raises the SCA to 119.4° ± 2.9°. However, as they undergo biofouling, the hydrophilicity of the UT membranes drastically increases, resulting in a SCA of 32.1° ± 11.7° after 500 hours. This is attributed to the hydrophilic nature of the polysaccharides, namely alginate[89], that comprise the majority of the ECM composition. The OLI membranes demonstrated markedly less loss in hydrophobicity, finishing with a SCA of 96.3° ± 10.9° after 500 hours. Hence, OLI membranes were able to maintain hydrophobicity due to limited biofilm formation, whereas UT membranes convert from hydrophobic to hydrophilic.

2.5 Discussion

As confirmed by fluorescence imaging and SCA measurements, OLI coated selectively permeable membranes demonstrated a reduced rate of biofilm formation and effectively maintained repellency. This finding is aligned with results obtained in similar biofouling studies

for OLI coatings on nonporous substrates[87,90–92]. When paired with the DO meter, OLI membranes provided superior long-term reproducibility, demonstrating a peak deviation in sensitivity of only 10.3% after 500 hours. We also prove that DO is capable of permeating the thin perfluorodecalin layer, and that the fluorosilane does not significantly disrupt the porosity and permeability of the membrane itself. It generally takes the meter between 10 and 15 minutes to give a stable reading in a given aliquot of water. This was the case for both UT and OLI membranes, and did not alter over the course of the experiment. Considering the minimal drop in contact angle on OLI membranes in **figure 2.4f**, the fluorosilane SAM was not compromised by significant corrosion or leaching that would have diminished the presence of hydrophobic fluorine on the surface.

A few setbacks with the OLI coating became apparent during the experiment. While the OLI coating was successful in suppressing the rate at which biofouling occurred, noticeable biofouling was observed using fluorescence microscopy after 100 hours, or 4 days. Epstein *et al.* demonstrated that an OLI coating was able to prevent over 95% of bacterial attachment for three different strains of bacteria over a 7-day incubation period[93]. However, in our work, the membranes were not incubated with individual strains of bacteria but rather numerous strains gained from the ambient air and tap water, which is more representative of practical applications. The heterogeneous distribution of the biofilms in fluorescence images indicate that formation occurred in favoured areas on the OLI membranes. This suggests that the fluorosilane SAM was likely unevenly distributed over the surface, and some areas may have lacked enough fluorosilane to effectively capture the lubricant. This is a pitfall of the LPD method that can be addressed by the chemical vapour deposition (CVD) of silanes[94]. However, CVD is more procedurally complex and putting the thin membranes under vacuum for extended time can

induce stretching, whereas the Extech DO sensor requires the membrane to be taunt against the electrode.

Going forward, there are a few parameters that need to also be investigated. During this experiment, the membranes were incubated in a non-flowing environment. While this can be considered representative of some smaller waterbodies such as ponds, swamps, or marshes, the majority of waterbodies exhibit substantial flow rates and patterns; this may impact the stability of the perfluorodecalin layer over time. In the case where water is very turbulent and the coating is exposed to higher concentrations of air bubbles, the perfluorodecalin may undergo evaporation due to its high volatility[95]. This could be addressed by periodic reapplication of perfluorodecalin or by considering more physically stable fluorinated oils, although it would need an equal or higher affinity to PFOTS. The stability of the lubricant layer or the fluorosilane SAM may also differ depending on the membrane material or porosity. For example, larger pores designated for other target molecules could enable the diffusion of perfluorodecalin. In this case, the lubricant could retreat through the membrane as a result of its hydrophobicity and leave an exposed fluorosilane SAM. On the other hand, smaller pores are at risk of being congested by fluorosilane during LPD and could render the membrane impenetrable.

In addition to water quality monitoring applications, our developed OLI coating offers strategic surface blocking for DO measurement in healthcare. Hypoxemia, the state of oxygen deficiency in arteries, is a symptom of numerous respiratory disorders and can lead to respiratory failure. Dissolved plasma oxygen (roughly 2% of the total oxygen in blood)[96] can be monitored by biosensors to evaluate the health of a patient[6] in a similar perspective to DO in natural waterbodies. However, alike to bacteria, blood is capable of interacting with unblocked surfaces. Through the contact coagulation cascade[61], clotted blood can cause pore blockages and

encapsulation of analyte that would diminish a device's reliability. In the case of bacterial infection in the bloodstream, which typically occur through the lungs or skin, biofouling may pose additional issues in the device design. OLI coatings are capable of simultaneously repelling bacteria and the plasma proteins responsible for coagulation[97]. This would enable a sensor to effectively measure DO concentrations in whole blood.

2.6 Conclusion

This work explored the application of OLI coatings on selectively permeable membranes and further justifies its use in preventing marine biofouling. In the context of a membrane-based DO sensor, a tethered liquid fluorocarbon OLI coating successfully suppressed the rate of biofilm formation over a three-week period. This enabled the DO sensor maintain its sensitivity and provide more accurate readings in comparison to unmodified membranes. These findings present an effective solution that addresses the wide use of selectively permeable membranes in sensing technologies and the need for antibiofouling strategies in numerous areas of research and commercial industries.

3. Prolonging Blood Coagulation during DNA Biosensing with a Novel Omniphobic Lubricant-Infused Coating

Matthew Osborne [a], Maryam Badv [a], Tohid F. Didar [a,b,c]

[a] School of Biomedical Engineering, McMaster University, Hamilton, Ontario, Canada

[b] Department of Mechanical Engineering, McMaster University, Hamilton, Ontario, Canada, Canada

[c] Institute for Infectious Disease Research (IIDR), McMaster University, Hamilton, Ontario, Canada

Author Contributions: MO was involved in the design and execution of all experiments and data analysis. TD was involved in the experimental design, supervised the project to completion, and provided all financial support. MB conducted the plasma coagulation assay with samples prepared by MO, and provided statistical analysis for the figures. MO wrote the manuscript with contributions from TD and MB.

3.1 Abstract

DNA biosensing is an integral aspect of point-of-care testing, and can detect a multitude of biomarkers for diagnosis and disease monitoring. However, non-specific binding of untargeted molecules on biosensing surfaces can lead to false positive diagnoses. Omniphobic lubricant-infused (OLI) coatings use a thin immobilized layer of slippery lubricant to prevent non-specific binding, while having also demonstrated anticoagulative capabilities. In this work, we have designed a biofunctional OLI coating with integrated DNA probes using carbon dioxide plasma activation treatment following the deposition of a fluorosilane monolayer. An optimal secondary CO_2 plasma treatment time of 2 minutes was found to sparingly etch a self-assembled monolayer of fluorosilane and simultaneously induce carboxyl groups for covalent immobilization of the DNA probe. This condition produced the highest fluorescence signal

relative to other treatment times, a contact angle of 76.3°, and a sliding angle of 10.8°. The DNA functionalized OLI coating significantly attenuated clot formation in a plasma coagulation assay when compared with surfaces coated with BSA or PLL-PEG. Using a DNA hybridization assay in human whole blood, biofunctional OLI exhibited a detection sensitivity equal to that of PLL-PEG blocked samples, and greater than that of BSA and unblocked samples. These findings show promising potential for the use of OLI coatings in DNA biosensing with human whole blood samples for point-of-care testing and wearable technologies that work with complex fluids.

Keywords: DNA; biosensor; microarray; omniphobicity; lubricant-infused; coating; anticoagulation; surface blocking; point-of-care testing

3.2 Introduction

In DNA biosensor design, both the bioreceptor and target biomarker are single-stranded nucleic acids (ssDNA). The bioreceptor is an oligonucleotide that can be referred to as the probe DNA (pDNA)[98–100]. When working with highly sensitive and cost-effective optical transducers (*e.g.* fluorescent tagging)[20], the pDNA is often immobilized on a substrate in microarrays[25]. These "gene chips" allow for parallel observation of optical signals, miniaturization, and multiplexing for different targets[101]. Capture occurs through complementary base pairing (*i.e.* hybridization), where a particular sequence on the pDNA binds to a matching sequence on the target DNA (tDNA). Targeted double-stranded DNA can be denatured using thermal (melting) and/or organic solvents (*e.g.* urea, formamide)[102,103]. Otherwise, microRNA can be targeted more directly since it is exclusively single-stranded *in vivo*, and it has been identified as a biomarker for multiple cancers in humans[104]. Both ssDNA and RNA oligonucleotides are more stable bioreceptors in comparison to protein bioreceptors, such as antibodies or enzymes, or cells[23,105]. Due to the ongoing work in DNA sequencing, pDNA can be designed and synthesised to detect

tDNA from a variety of origins (*e.g*. bacterial, viral, and eukaryotic). Hence, DNA biosensors have a broad range of applications in point-of-care testing, including detection of bacterial infections[106,107], viruses[108,109] and cancer[110–112].

When designing a DNA microarray, non-specific binding (NSB) of untargeted molecules on the substrate's surface must be minimized to optimize specificity and prevent false positive diagnoses[113]. Therefore, chemically inert blocking agents must be immobilized on potential binding sites unoccupied by pDNA. This is accomplished using either physisorption or chemisorption. Chemisorption is the most preferable due to the higher strength of covalent bonds in comparison to Van-der-Waals and other electrostatic interactions[114]. Bovine serum albumin (BSA) is a protein blocking agent long implemented in immunochemical assays like ELISAs and Western blots because of its relatively small size, stability, and non-reactivity, although BSA has been known to react with some human antibodies[35,115]. Polyethylene glycol (PEG) is the most common polymer for preventing NSB and is considered to be a highly versatile and effective blocking agent[30]. It is usually grafted to other polymers such as poly-l-lysine (PLL) to increase the strength of electrostatic adsorption, but this is at higher synthesis complexity and cost[41,116,117]. The aforementioned conventional blocking agents are physically adsorbed to surfaces after bioreceptor immobilization, meaning that they are prone to desorption over time or in varying conditions (*e.g.* temperature, pH, flow rate).

Omniphobic lubricant-infused (OLI) coatings are an emerging class of highly repellent and slippery surface modifications inspired by the *Nepenthes* pitcher plant[97]. Microstructures on the pitcher rim are capable of maintaining a thin layer of water from rainfall to create a low friction environment, causing prey to "aquaplane" into the pitcher[53]. Similarly, OLI coatings immobilize a thin layer of lubricant and when another fluid is applied to the surface, the resulting

liquid-liquid interface is extremely slippery (sliding angles of ~5°)[118]. The term "omniphobic" is used since these coatings have been proven to repel both water-based (hydrophobic) and oil-based (oleophobic) solutions[119]. To achieve a liquid-liquid interface, micro- or nano-scale features must be present so that the lubricant maintains a higher affinity to the coated surface than the working solution. These features can be geometrical and/or chemical in nature. Geometrical features (*i.e.* surface texturing) can provide a physical affinity to lubricants but require expensive fabrication techniques, namely photolithography, and specialized materials[55,57,58,120]. Alternatively, liquid phase deposition (LPD) or chemical vapour deposition (CVD) can be used to coat molecules with high molecular affinity to specific lubricants onto the substrate's surface[62]. Between the two methods, CVD offers a more homogeneous distribution, cleaner finish, and produces less waste[121]. Silanes with fluorocarbon chains, commonly referred to as fluorosilanes, have demonstrated a suitable affinity to anhydrous fluorinated lubricants for use in OLI coatings[122].

OLI coatings have proven to be an effective tool in limiting the rate of blood coagulation[61,123,124]. The contact (intrinsic) pathway for blood coagulation requires the adsorption of three plasma proteins on artificial surfaces: factor XII (Hageman factor), plasma prekallikrein, and high molecular weight kininogen[125,126]. This subsequently triggers the activation of other factors and fibrin crosslinking, which produces a surface-bound blood clot. Blood clots may block open bioreceptors and entrap targeted biomarkers, while the very numerous and varying elements of whole blood risk non-specifically interacting with the biointerface. Hence, by reducing bioreceptor-biomarker interactions and increasing NSB, whole blood tends to diminish the sensitivity and specificity of the biosensor[127,128]. The self-cleaning repellency of OLI coatings

diminishes the adsorption of plasma proteins to prolong the initiation of the coagulation cascade and enable more bioreceptor-biomarker binding to occur.

In this work, we introduce a novel process to integrate pDNA with the OLI coating (**figure 3.1**) to enhance the sensitivity and specificity of tDNA capture in human whole blood while leveraging the coating's surface blocking and anticoagulative properties. To achieve this, amine-labeled pDNA are immobilized on a fluorosilane-coated glass surface using carbon dioxide plasma activation and EDC/NHS, an established crosslinking strategy for biomolecular immobilization[129]. Once fabricated, we assessed the biofunctional OLI coating's ability to prolong blood clot formation, and compared its impact on tDNA detection in blood to two conventional blocking agents: BSA and PLL-PEG.

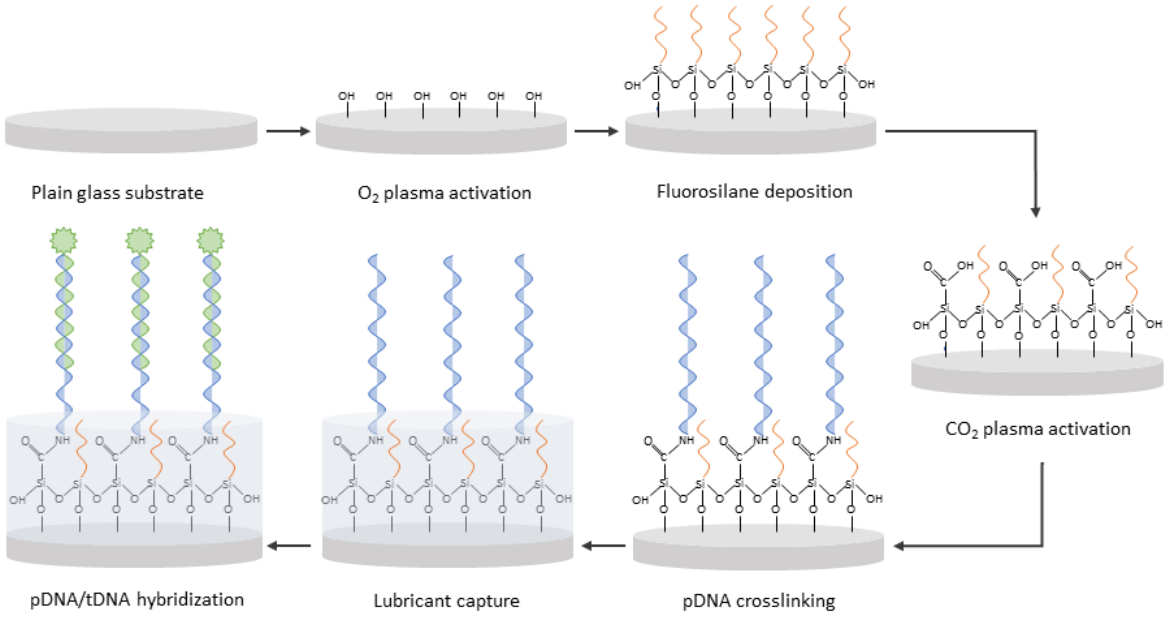

Figure 3.1. Flow diagram for two-part pDNA functionalization of omniphobic liquid-infused glass surfaces. Oxygen plasma activation is used to induce hydroxyl groups on the surface of a plain glass substrate. Fluorosilane is deposited onto the substrate using CVD and forms a self-assembled monolayer (SAM). Carbon dioxide plasma activation is used to etch

some carbon-fluorine chains (orange), and simultaneously induce carboxyl groups. Amine-labeled pDNA (blue) is covalently bound to these carboxyl groups using EDC/NHS. Perfluorodecalin lubricant is added to the surface and a thin layer is immobilized by the remaining fluorosilane molecules. Fluorescein-labeled tDNA (green) hybridizes with the immobilized probes but is unable to physically adhere to the blocked surface. This figure is not drawn to scale to better illustrate the progression of the surface chemistry.

3.3 Methods

Materials. Glass microscope slides, 48-well plates, and buffered sodium citrate blood collection tubes were purchased from VWR (Mississauga, Canada). Trichloro (1H,1H,2H,2H-perfluorooctyl) silane (PFOTS), 2-(N-morpholino) ethanesulfonic acid (MES), 1-ethyl-3-(3-dimethylaminopropyl) carbodiimide (EDC), N-hydroxysuccinimide (NHS), bovine serum albumin (BSA), 4-(2-hydroxyethyl)-1-piperazineethanesulfonic acid (HEPES), and perfluorodecalin was purchased from Sigma-Aldrich (Oakville, Canada). $CaCl_2$ and saline-sodium citrate (SSC) were prepared in-house. Poly(L-lysine)-g[3.5]-polyethylene glycol (PLL-PEG) was purchased from Susos Surface Technology (Dubendorf, Switzerland). All sets of oligonucleotides (**Figure SI 3.1**) were purchased from Integrated DNA Technologies (Skokie, USA). Human whole blood and plasma was collected in the buffered sodium citrate blood collection tubes by donation from healthy volunteers, pending their written consent, and approved by the Hamilton Integrated Research Ethics Board.

Oxygen plasma activation. Oxygen plasma activation simultaneously etches the surface of the glass and induces hydroxyl groups, which are available for covalent immobilization[130]. Plain glass microscope slides were treated in a Harrick PDC-001 (115V) plasma cleaner for 3 minutes at a pressure of 450 mTorr.

Chemical vapour deposition. Immediately after activation, the samples are transferred to a vacuum desiccator with 200 µL PFOTS. CVD is performed at 20 kPa for 2 hours. The PFOTS evaporates and gradually forms a SAM on the exposed glass surfaces. PFOTS covalently binds with the activated hydroxyl groups and surrounding PFOTS groups, releasing hydrochloric acid as a by-product. Samples are subsequently baked on a hot plate at 100°C for a minimum of 6 hours to promote bond formation and evaporation of hydrochloric acid. Samples are washed vigorously with distilled water for 30 seconds to remove unbound PFOTS.

Carbon dioxide plasma activation. Similar to oxygen plasma, carbon dioxide plasma activation simultaneously etches the surface and induces functional groups, which have been previously shown to include carboxyl, aldehyde, ketones, esters, and hydroxyl groups[131]. Since a second plasma activation etches the existing fluorocarbon chains, we looked for an optimal CO_2 plasma activation time at 600 mTorr to induce carboxyl groups on PFOTS SAMs (**figure 3.2** and **figure 3.3**).

X-ray photoelectron spectroscopy (XPS). Samples were prepared with PFOTS and varying amounts of CO_2 plasma activation time (0 minutes, 30 seconds, 1 minute, 2 minutes, 3 minutes). Plain glass samples with and without 3 minutes of CO_2 plasma activation were also prepared. Survey and high-resolution spectra were obtained from a Thermo Scientific K-Alpha XPS System at Surface Interface Ontario, University of Toronto.

DNA microarray printing. 100 µM pDNA was diluted to 5 µM in 0.1 M MES buffer at pH 4.5 with 0.2 M EDC and 0.2 M NHS. A Scienion SciFlexArrayer S5 non-contact microarray printer was used to print 9 nL droplets of the mixed pDNA solution in 850 x 850 µm spaced grids on each sample. EDC activates the carboxyl groups etched into the PFOTS SAM and enables the amine-labeled pDNA to covalent bind to them. Samples were placed in a 70% humidity chamber

and left to incubate for a minimum of 4 hours. They were then rinsed with distilled water for 10 seconds to remove unbound pDNA.

DNA hybridization in buffer. 100 µM tDNA was diluted to 1 µM in 1X SSC buffer at pH 7.0. Samples were saturated in perfluorodecalin for 2 minutes. Immediately after removing the excess lubricant, 40 µL drops of the mixed tDNA solution were added to each sample and incubated in a dark environment for 3 hours. Samples were rinsed with distilled water for 10 seconds. Images were obtained with a Zeiss AX10 inverted microscope with ApoTome.2 fluorescence functionality. Fluorescence intensity was quantified using ImageJ image processing software. The 2 highest and lowest values were removed for each condition. There are 18 complementary base pairs between the selected pDNA and tDNA.

Static contact and sliding angle measurements. Static contact angle (SCA) measurements were taken using a Future Digital Scientific Corporation OCA 35 contact angle meter on air-dried samples with 5 µL droplets of deionized water. Sliding angle measurements were taken using a goniometer with 5 µL droplets of deionized water immediately after samples were saturated in perfluorodecalin for 1 minute.

Plasma coagulation assay. Samples were prepared in a 48-well plate. Instead of microarray printing, 10 µL of 5 µM pDNA drops were added by hand to each surface. BSA samples had 10 µL of 1% BSA in deionized water by weight added to each unblocked surface after pDNA immobilization and were incubated for 1 hour. PEG samples had 10 µL of 4.5 µM PLL-PEG in 1X PBS added to each unblocked surface and were incubated for 1 hour. Samples with fluorosilane were saturated in 100 µL of perfluorodecalin for 5 minutes before removing the excess lubricant. Immediately after, 100 µL of citrated human plasma was added to each well and incubated at 37°C for 10 minutes. Meanwhile, 1 M $CaCl_2$ was diluted to 25 mM in 20 mM

HEPES buffer at pH 7.4, and 100 µL of this solution was added to all wells to initiate clotting. The absorbance at 405 nm of each well were measured at 8-second intervals in using a SPECTRAmax plate reader (Molecular Devices). The half-time to clot was defined as the time required to reach the half-maximum absorbance as read by the plate reader.

DNA capture in whole blood. Samples were prepared with 1 µL of 5 µM pDNA drops added by hand. BSA and PEG samples were blocked using the same method described in the plasma coagulation assay. 100 µM tDNA and 100 µM non-complementary (ncDNA) were diluted to 2 µM each in 5 mM $CaCl_2$. Samples with fluorosilane were saturated in perfluorodecalin for 5 minutes before removing the excess lubricant. 10 µL droplets of citrated blood was added to each surface and 10 µL of the tDNA solution was immediately pipetted into each blood droplet. Samples were left to hybridize and clot for 2 hours, then washed with distilled water for at least 10 seconds or until the clot is removed. Images were taken using the Zeiss AX10 inverted microscope and analyzed using ImageJ.

Statistical analysis. Data are presented as means ± standard deviation. Statistical significance was assessed using analysis of variance and post-hoc analysis with Tukey's test, where significant difference was considered as $P < 0.05$.

3.4 Results

To first assess the viability of immobilizing pDNA on a fluorosilane SAM, XPS analysis was used to compare the simultaneous increase in carboxyl groups and loss of fluorine with CO_2 plasma activation time. Survey spectra (**figure 3.2a**) were used to quantify the elemental distribution for each configuration. As expected, a decrease in fluorine is observed with increasing CO_2 plasma activation time and surface etching. Meanwhile, the presence of oxygen

increases as various oxygen-based functional groups are induced on the surface. The increase in carbon is relatively small since the induction of carboxyl groups is simultaneously offset by the partial etching of some fluorocarbon chains. Finally, silicon also increases with CO_2 plasma activation time. This can be attributed to the complete etching of some fluorocarbon chains, exposing the silicon atom at the base of the silane. Analysing high-resolution carbon spectra at peak binding energies between 288.5 eV and 289.0 eV (**figure 3.2b**) confirms that carboxyl groups become exponentially more prevalent on samples that have undergone longer CO_2 plasma activation times. Carboxyl groups make up 13.0% ± 1.6% of the total carbon bonds on surface of the fluorosilanized glass after 3 minutes of CO_2 plasma activation, whereas non-silanized glass at 3 minutes was the optimal configuration for inducing carboxyl groups at 19.6% ± 2.1%.

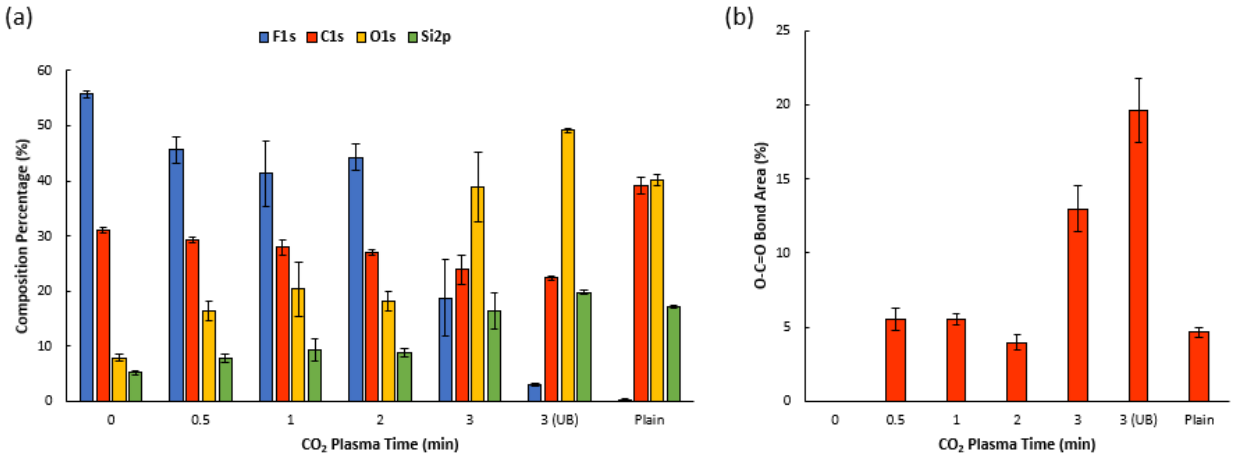

Figure 3.2. XPS characterization of fluorinated glass surfaces with increasing CO_2 plasma activation time. (a) Survey spectra of fluorosilane-coated glass surfaces show a decrease in fluorine and increases in oxygen, carbon, and silicon with increasing CO_2 plasma activation time. (b) High-resolution carbon spectra confirm an increase in surface carboxyl groups with CO_2 plasma activation time, which will be used for pDNA immobilization.

The simultaneous induction of carboxyl groups and loss of fluorine was further verified with the immobilization of pDNA on fluorosilanized samples and its subsequent hybridizing with fluorescein-labeled tDNA in buffer (**figure 3.3a**). Controls included a 3-minute CO_2 activated unblocked glass surface (UB), and a plain glass surface with no functional groups available for crosslinking. As plotted in **figure 3.3b**, the fluorescence intensity of hybridized spots increases with CO_2 plasma activation time until 2 minutes. This again confirms that more carboxyl groups are available for pDNA to bind with, which increases the surface density of pDNA. Unmodified fluorosilanized glass surfaces showed negligible fluorosilane since the perfluorodecalin layer prevents tDNA from hybridizing with any non-specifically bound pDNA, which lack the vertical orientation needed to permeate the lubricant. The 3-minute fluorosilane and unblocked conditions exhibited a decrease in fluorescence intensity in comparison to 2 minutes of CO_2 plasma activation time. This suggests that the additional increase in carboxyl groups from 2 to 3 minutes is no longer able to account for the total increase in surface area (**figure 3.3c**), and there is a net decrease in pDNA surface density.

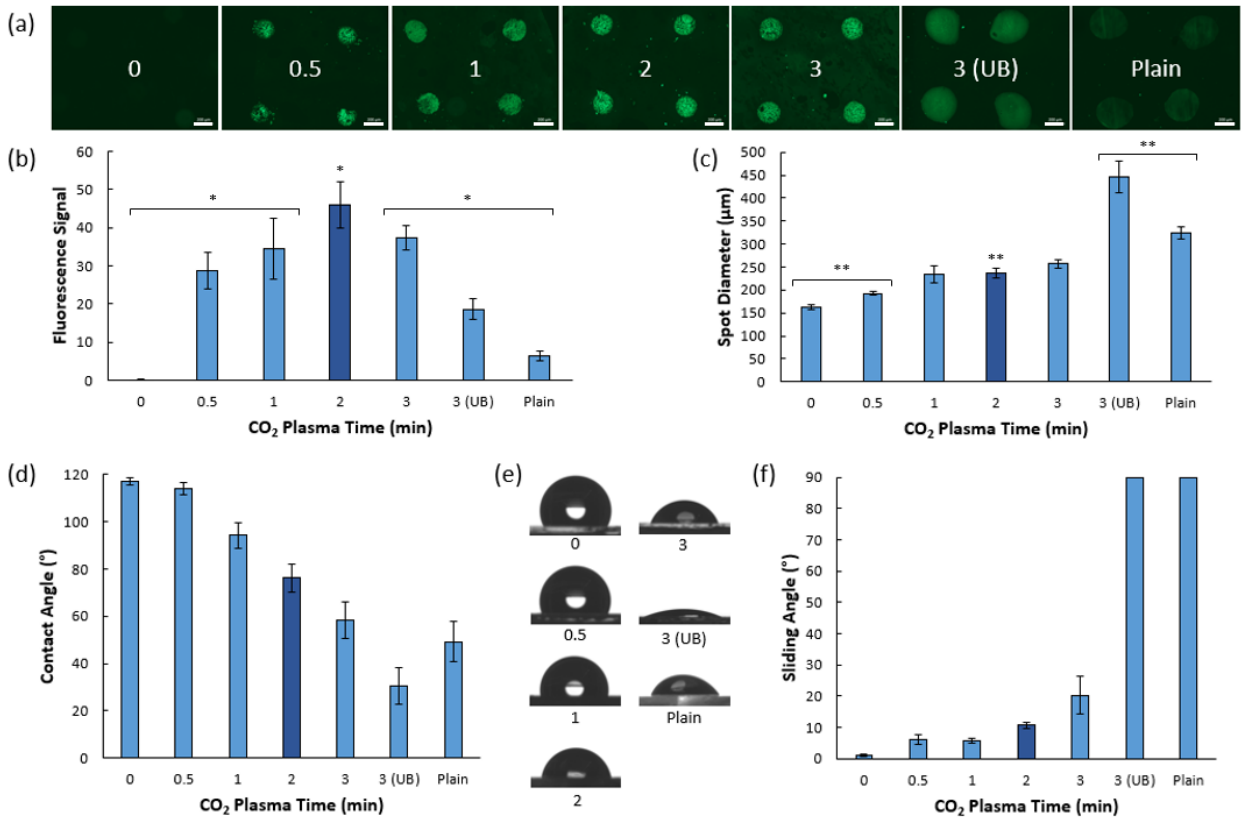

Figure 3.3. DNA microarray after hybridizing with fluorescein-labeled tDNA in buffer. (a) Fluorescence images of DNA microarray spots at different CO_2 plasma activation times. Non-fluorinated glass with and without 3 minutes of CO_2 plasma are used as controls. Scale bar = 200 µm. (b) The fluorescent signal is defined as the fluorescence intensity of the microarray spots minus the fluorescent intensity of the background. This value increases with CO_2 plasma activation time until 2 minutes. Samples with fluorosilane exhibit a significantly higher fluorescence signal compared to the controls. *Significant difference in fluorescent signal between the 2-minute samples and all other conditions ($P < 0.05$). (c) The microarray spots show an increasing diameter with increasing CO_2 plasma activation time. The controls have significantly higher spot diameters (> 320 µm) than the samples with fluorosilane (160-260 µm). **Significant difference in spot size between the 2-minute samples and the 4 indicated

conditions ($P < 0.001$). (d, e) Static contact angle measurements show a decrease in hydrophobicity with increasing CO_2 plasma activation time. Samples can no longer be considered hydrophobic after 1 minute of CO_2 plasma. (f) Sliding angle measurements demonstrate that all fluorinated samples provided a significant degree of slipperiness, but samples became less slippery with increasing CO_2 plasma activation time. No sliding was observed on the controls.

Next, the repellency of the OLI coating was quantified using two conventional tests. SCA measurements (**figures 3.3d-e**) demonstrated a consistent decrease in surface hydrophobicity (*i.e.* increase in hydrophilicity/surface energy) with increasing CO_2 plasma activation time. This corresponds directly with the decrease in fluorine observed using XPS. Hydrophobic substrates are characterized as exhibiting a SCA of 90° or higher. Therefore, fluorosilane-treated samples are hydrophobic up to 1 minute of CO_2 plasma activation (94.3° ± 5.4°), whereas samples treated for 2 minutes (76.3° ± 5.8°) are considered to be mildly hydrophilic. Intuitively, the SCA is inversely correlated to the spot size, and this is supported by inverted trends depicted in **figure 3.3c** and **figure 3.3d**.

Sliding angle measurements (**figure 3.3f**) showed that all samples with fluorosilane had significantly low sliding angles, implying high slipperiness and repellency. Among these samples, the sliding angle peaked at 3 minutes (20.3° ± 6.1°), roughly twice that of 2 minutes (10.7° ± 1.1°) and four times that of 1 minute (5.8° ± 0.9°). This decreasing trend in repellency reaffirms the fluorosilane SAM's gradual forfeiture of its ability to lock the lubricant to the surface due to plasma etching. Samples without fluorosilane, with and without CO_2 plasma activation, failed to show any sliding up to a vertical 90° inclination.

The time consumption of POC testing can be minimized by working directly with whole blood samples taken from the patient rather than first processing the blood to filter out undesirable components (*e.g.* cells and platelets). Filtering adds procedural steps and time, and risks accidentally lowering the tDNA concentration if done inefficiently. However, as previously mentioned, working with whole blood can be detrimental to the sensitivity and specificity of the biosensor. Therefore, the performance of OLI coated DNA biosensors in human whole blood was weighed alongside conventional blocking agents, PLL-PEG and BSA. To assess each blocking agent's ability to slow the rate of plasma clotting, each sample was submerged in citrated human plasma in an individual well. A 25 mM $CaCl_2$ solution was added to the wells using a multichannel pipette to simultaneously induce clotting. As shown in **figure 3.4**, OLI coated DNA biosensors extended the time taken to reach half-maximum clotting, as characterized by each well's absorbance, to 369 ± 8 seconds, which is not significantly different to the optimal condition of blank wells (379 ± 45 s). OLI coated DNA biosensors significantly outperformed PLL-PEG (288 ± 18 s), BSA (265 ± 14 s), and full DNA coverage (310 ± 28 s). It can be concluded that OLI coated DNA biosensors provide an optimal and consistent attenuation of plasma clotting.

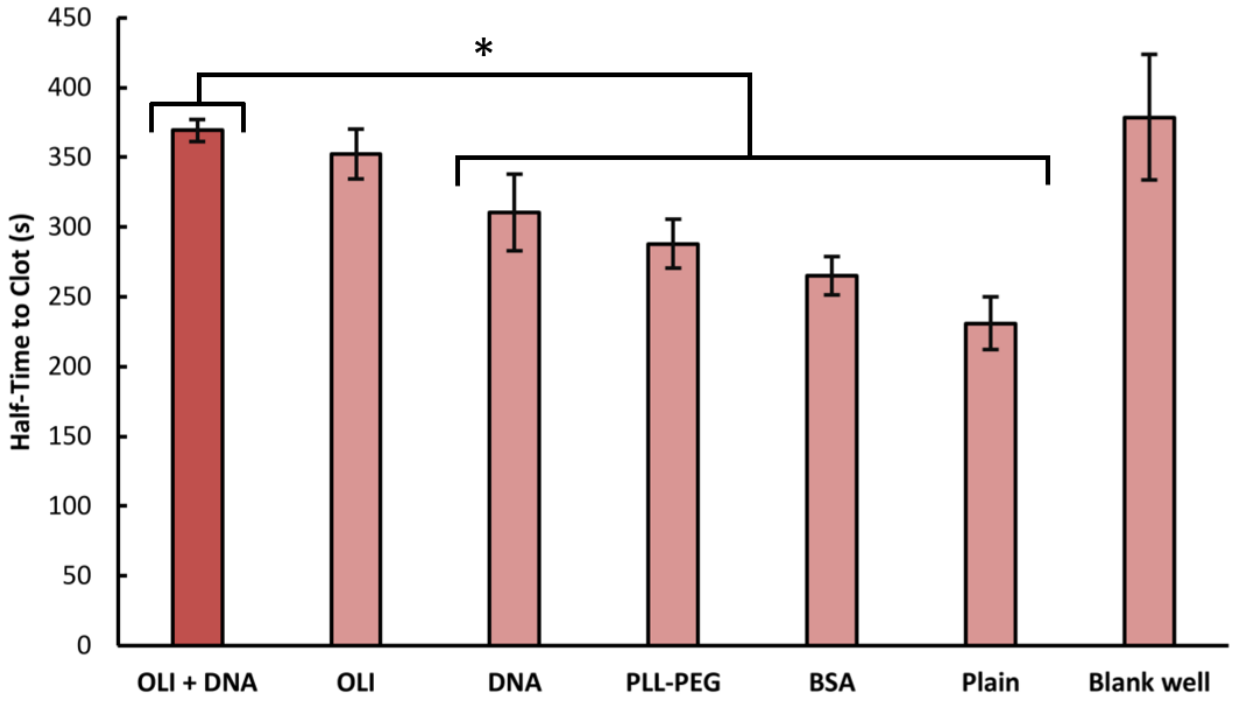

Figure 3.4. Clotting times of various surface blocking conditions for an induced plasma coagulation assay. The OLI coated DNA biosensors outperformed PLL-PEG blocked, BSA blocked, and unblocked glass surfaces in elongating the plasma clotting time, as per an absorbance-based coagulation assay. The developed coating performs on par with blank wells, which is considered the optimal control for this assay. *Significant difference in clotting times between the OLI + DNA samples and the 4 indicated conditions ($P < 0.05$).

Once the antithrombogenic properties of this novel coating were established, we investigated the effect it would have on capturing tDNA in whole blood, again comparing it against PLL-PEG, BSA, and UB surfaces. Both tDNA and non-specific ncDNA (control), labeled with green and red fluorophores respectively, were diluted in the same $CaCl_2$ solution. A droplet of equal parts of citrated whole blood and $CaCl_2$ solution was added to each surface and simultaneous clotting and hybridization was allowed to occur for 2 hours of incubation. **Figure 3.5** shows that the OLI and PLL-PEG samples exhibited the highest fluorescence intensities,

followed by BSA and unblocked. As expected, all fluorescence intensities were significantly less than the OLI and UB readings obtained from hybridization in buffer, confirming that coagulating blood attenuates tDNA capture. The ncDNA reveals the amount of NSB that occurs in the pDNA region, and should be accounted for when analysing the fluorescent reading. Hence, a significant difference between tDNA and ncDNA intensities is critical. In the case of BSA blocked and UB surfaces, this difference is not significant, thus signifying that the reading itself is unreliable.

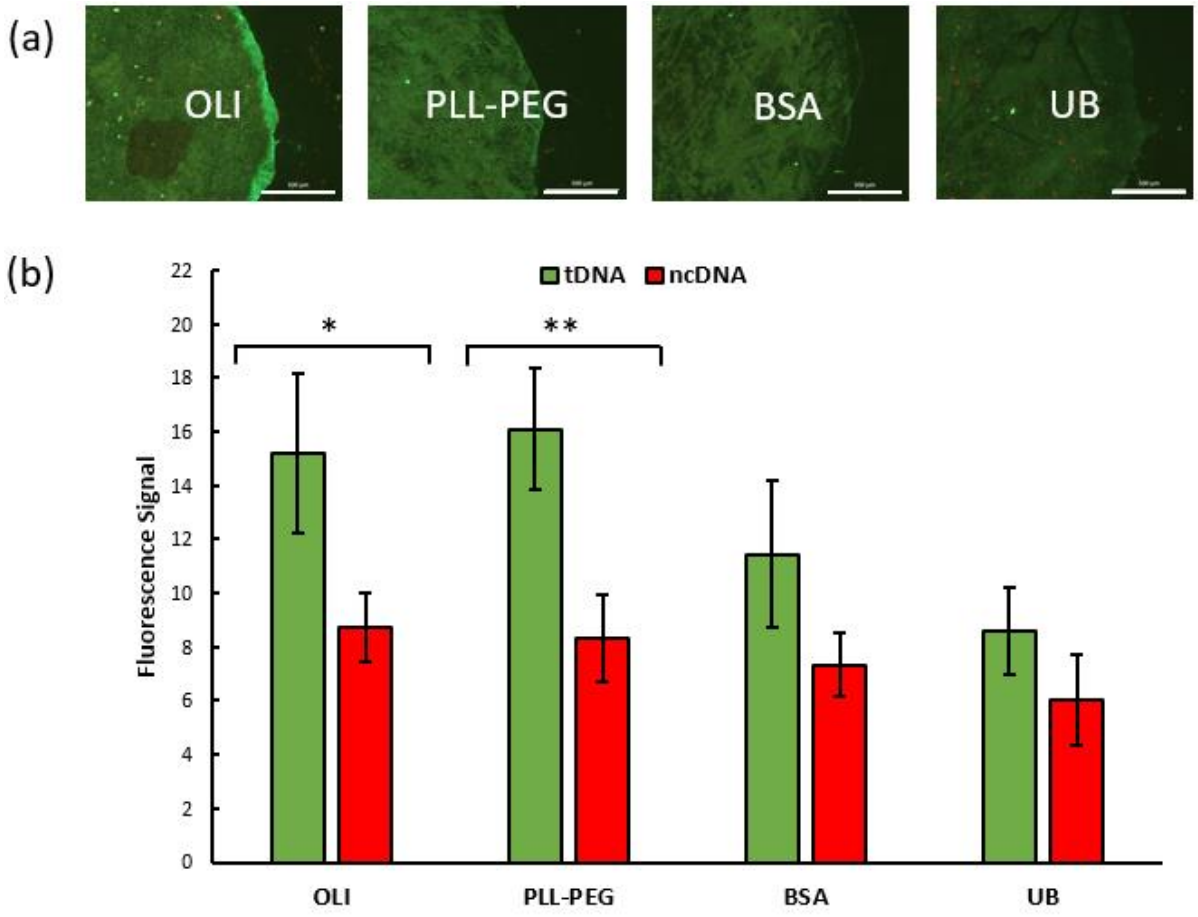

Figure 3.5. Capturing tDNA in whole blood. (a, b) OLI coated DNA biosensors produce a higher fluorescent signal in response to capturing fluorescein-labeled tDNA (green) in comparison to BSA blocked and unblocked DNA biosensors, and performs on par with PLL-PEG blocked samples. Non-specific adhesion of ncDNA (red) is similar amongst all four

blocking conditions. Scale bar = 500 µm. *, **Significant difference in fluorescent signal between the tDNA and ncDNA ($P < 0.05$).

As alluded to earlier with the higher hydrophobicity of the OLI coating, the surface area for DNA interaction is smaller. This means that the surface density of both tDNA and ncDNA interactions is higher. Non-slippery hydrophobic surfaces would exhibit more NSB due to the higher surface density of ncDNA, but the slippery repellency of the OLI coating also deters NSB. These phenomena appear to cancel each other out since the ncDNA fluorescence intensities are low in all four conditions.

3.5 Discussion

Our work has successfully established an optimal balance of OLI repellency with pDNA functionality. A CO_2 plasma activation time of 2 minutes was used to sparingly etch the surface of a fluorosilane SAM and induce a high surface density of functional binding sites for pDNA immobilization. The pDNA were synthetically designed to capture complementary tDNA. Furthermore, the OLI coating's hydrophobicity and anticoagulant properties enable these DNA biosensors to successfully capture tDNA in whole human blood with comparable sensitivity to PLL-PEG coated biosensors and higher than BSA or unblocked equivalents. Blood is a complex biological solution with higher viscosity and heterogeneity than typical buffers, leading to more complications in analysing its composition. The addition of fluorosilane SAM and perfluorodecalin has been proven to extend the time needed for the blood to clot on DNA biosensors by 19.0%.

There are several elements of the current design that are advantageous. As mentioned earlier, the hydrophobicity of these surfaces results in a higher pDNA surface density and

fluorescent signal. Moreover, pDNA droplets were able to hold their circular shape during immobilization, resulting in more clearly defined spots and aligned surface patterning. On the other hand, pDNA droplets on hydrophilic surfaces were drawn out across the surface and formed more amorphous shapes. The hydrophilic surfaces also posed a higher risk of droplet agglomeration during printing, therefore the grid spacing for hydrophilic surfaces must be kept larger than hydrophobic surfaces. Since PFOTS is a relatively small molecule (480 Da) and the pDNA is immobilized on top of the partially etched SAM, shorter oligonucleotides are highly accessible for hybridization. In the case of PLL-PEG (22 kDa) and BSA (66 kDa), steric interactions between the blocking agent and the 33bp pDNA (10.5 kDa) is more likely to interfere with the hybridization process, particularly if the surface density of the blocking agent is too high.

In terms of fabrication, these biosensors can be prepared in less than 12 hours and the surface blocking comes at a comparable cost ($8.40 per 100 samples) to PLL-PEG ($6.00 per 100 samples) (**Figure SI 3.2**). The only specialized equipment required are a plasma cleaner and a desiccator, which can be substituted for cheaper alternatives such as piranha solution and LPD, respectively. The OLI-coated biosensors are also designed for longer stability in storage. The fluorosilane SAM is covalently bound to the surface and stable in ambient or refrigerated temperatures. Perfluorodecalin is stored in a sealed container and can be added to the surface immediately before use. PLL-PEG and BSA, however, are bound via physisorption and are prone to detach from the surface without notice.

When designing for a specific application, a number of components in the current design would need to be re-evaluated. The primary reasons for selecting glass as the substrate are its low cost, availability, consistent and smooth surface, and favourable optical properties,

specifically a low background fluorescence. However, it is highly brittle and difficult to cut. A variety of low-density polymer substrates may be more suitable for applications in wearable or geometrically-intricate devices. OLI coatings have already been implemented on: polystyrene, polycarbonate, polysulfone, polypropylene, titanium, silicon wafer, and polytetrafluoroethylene[97]. PFOTS is relatively inexpensive and effective at self-assembly after surface oxidation. Yet, it is water insoluble and highly corrosive, making it difficult and dangerous to work with in its natural state. Perfluorodecalin is a relatively inexpensive and FDA-approved lubricant with a proven affinity to PFOTS, but it too has a high vapour pressure of 6.25 torr and evaporates under standard atmospheric conditions. When applied to the fluorosilane SAM, thin layers of perfluorodecalin must be quickly isolated from the atmosphere as it is capable of evaporating within a minute. Instead, fluorinated lubricants with higher vapour pressures (*e.g.* perfluoroperhydrophenanthrene, < 1 torr) can be used in open environments at a reduced rate of evaporation but usually at increased cost, reduced affinity, or chemical risks. When designing the pDNA sequence, longer complementary sequences result in higher specificity and melting temperatures (*i.e.* bond stability) from the increased number of hydrogen bonds[132]. However, longer pDNA molecules risk interacting with one another or folding upon themselves, which would make them incapable of hybridizing with tDNA. Hence, an optimal pDNA length for this coating still needs to be investigated.

While the current design is limited to single-stranded nucleic acid detection, the pDNA oligonucleotides can be substituted with amine-labeled DNA aptamers or DNAzymes to expand detection capabilities to proteins and cells. Aptamers are synthetic oligonucleotides with protein-binding capabilities and can interact with whole cells through their transmembrane proteins[133]. Fluorescently-labeled or colorimetric reporter aptamers can be subsequently used to recognize

biomarker capture. Moreover, DNAzymes are aptamers with catalytic functionality that produce chemical signals upon detecting biomarkers without the use of an additional reporter molecule[134]. Considering that any amine-terminating biomolecule can be crosslinked to the EDC-activated carboxyl groups, the flexibility of this coating design is suitable for an extensive variety of biomarkers in point-of-care testing.

The slippery aspect of this OLI coating poses a considerable advantage for digital microfluidics. In this area of research, discrete droplets of sample are manipulated on a surface using an array of electrodes[135]. Droplets can be easily moved, divided, or merged to perform specific analytical tasks. The OLI coating has been shown to minimize the friction between aqueous droplets and coated substrates, enabling smoother droplet translation and reducing the voltage necessary for movement[136]. As proven in this work, it would also attenuate thrombotic activity between blood droplets and the device surface. Since the more hydrophilic pDNA penetrate the hydrophobic lubricant layer, surface patterning would be effective at capturing the droplets in specific locations for compartmentalized analysis or reactions.

3.6 Conclusion

We have developed a novel OLI coating with integrated pDNA bioreceptors. An optimal balance of repellency and functionality was established using 2 minutes of CO_2 plasma activation to simultaneously etch a fluorosilane SAM and induce carboxyl groups available for covalent attachment. The coating successfully attenuates blood coagulation and enables tDNA capture in whole blood at a comparable sensitivity to PLL-PEG, a gold standard of surface blocking. Its omniphobicity increases the surface density of pDNA immobilization and tDNA interactions, resulting in a higher sensitivity. Considering that the flexibility of the design

enables biosensing components to be easily substituted to address specific applications, the OLI coated DNA biosensor holds many advantages for faster and more effective point-of-care testing.

3.7 Supplemental Information

Function	Base Pairs	Label	Sequence
pDNA	33	Amino	5'-/5AmMC12/TT TTT TTT TTA GGA AGA AGT TTC AAG GAA AGG A-3'
tDNA	23	Fluorescein	5'-/56-FAM/TC CTT TCC TTG AAA CTT CTT CCT-3'
ncDNA	23	TEX 615	5'-/5TEX615/TG ACT GCA GTC ACG GAT CCT GAC-3'

Figure SI 3.1. Oligonucleotides used in the fabrication of OLI coated DNA biosensors and subsequent experiments.

Blocking Agent	Cost per 100 Samples
OLI (PFOTS + perfluorodecalin)	$8.40
PLL-PEG	$6.00
BSA	$0.22

Figure SI 3.2. Cost estimate for different blocking agents per 100 samples used in experiments.

4. Conclusion

This thesis has investigated the self-cleaning capabilities of omniphobic lubricant-infused coatings, and how these capabilities can be leveraged in biosensor design. In chapter 1, the biosensor was divided into several components. Different design approaches were explored with respect to their impact on biosensor performance, with emphasis on sensitivity, selectivity, and stability, as well as its feasibility of implementation in clinical and commercial settings. In chapters 2 and 3, the following outcomes were achieved:

- An OLI coating was applied on a selectively permeable membrane for dissolved oxygen and did not significantly alter the pre-biofouling sensitivity (2.3% deviation) of the DO sensor.
- The DO sensor's stability with coated and unmodified membranes was evaluated over a three-week period, and the OLI membrane maintained its sensitivity more effectively (10% deviation) than its counterpart (26% deviation).
- The OLI coating successfully curbed biofilm formation over the three-week period, as demonstrated by fluorescence microscopy, SEM, and SCA measurements.
- A novel coating was designed to optimize the balance of omniphobic repellency (76° SCA, 10° sliding angle) and DNA biosensing functionality.
- The OLI DNA biosensor elongated the rate of blood coagulation by 19% in comparison to an unblocked DNA biosensor.
- This design was capable of capturing tDNA at a comparable efficiency to PLL-PEG, the gold standard of surface blocking, and more efficiently than BSA and unblocked surfaces.

4.1 Future Work

Future work will focus on improving integration strategies for OLI biosensors. Further research will be conducted on pairing the novel biofunctional coating with different bioreceptors and transducers. DNAzymes offer near-instantaneous optical or chemical signals without the use of reporter molecules, and expand a biosensor's functionality to include protein or even whole-cell biomarkers. They can be labeled with functional groups for immobilization similar to the synthetic oligonucleotides used in chapter 3. Hence, DNAzymes are the next logical step in improving the integration and biofunctionality of the novel coating. Otherwise, due to the expensive and time-consuming nature of DNAzyme synthesis, this coating can be paired with electrochemical transducers for nucleic acid biosensing. In particular, the impact of the coating process on different electrode materials (*e.g.* gold, graphite, platinum) will be assessed to eliminate the need for reporter molecules and emphasize integration. To validate applicability in POC testing, new renditions of the coating should be used to test for the natural biomarkers of specific diseases, rather than synthetic targets. In addition to human blood, the biofunctional OLI coating will be investigated in conjunction with other complex fluids that pose issues of solidification, corrosion, and/or high viscosity (*e.g.* waste water, milk, urine, and saliva).

Within the broader field of micro total analysis systems, including lab-on-a-chip and organ-on-a-chip technologies, other topics of interest include the manipulation of blood droplets on slippery surfaces with patterned bioreceptor sites, and the impact of frictionless microfluidic channels on biofouling and coagulation. This could also be advantageous for working with shear-sensitive materials such as cells or non-Newtonian fluids. With these many research avenues in mind, the future of OLI coatings in biosensing looks to be both widespread and clinically valuable.

References

1. Canadian Institute for Health Information (CIHI). National Health Expenditure Trends. (2018).
2. Canadian Institute for Health Information (CIHI). Commonwealth Fund Survey 2016. (2017). Available at: https://www.cihi.ca/en/commonwealth-fund-survey-2016.
3. Government of Canada. Water: frequently asked questions. (2018). Available at: https://www.canada.ca/en/environment-climate-change/services/water-overview/frequently-asked-questions.html.
4. Government of Canada. Water pollution: causes and effects. (2010). Available at: https://www.canada.ca/en/environment-climate-change/services/water-overview/pollution-causes-effects.html.
5. Singh, R. *et al.* Biosensors for pathogen detection: A smart approach towards clinical diagnosis. *Sensors and Actuators, B: Chemical* **197,** 385–404 (2014).
6. Vashist, S. K., Luppa, P. B., Yeo, L. Y., Ozcan, A. & Luong, J. H. T. Emerging Technologies for Next-Generation Point-of-Care Testing. *Trends in Biotechnology* (2015). doi:10.1016/j.tibtech.2015.09.001
7. Zhuiykov, S. Solid-state sensors monitoring parameters of water quality for the next generation of wireless sensor networks. *Sensors and Actuators, B: Chemical* (2012). doi:10.1016/j.snb.2011.10.078
8. Liu, Y., Islam, M. A. & Gao, J. Quantification of shallow water quality parameters by means of remote sensing. *Prog. Phys. Geogr.* (2003). doi:10.1191/0309133303pp357ra
9. Glasgow, H. B., Burkholder, J. M., Reed, R. E., Lewitus, A. J. & Kleinman, J. E. Real-time remote monitoring of water quality: a review of current applications, and advancements in sensor, telemetry, and computing technologies. *J. Exp. Mar. Bio. Ecol.* (2004). doi:10.1016/j.jembe.2004.02.022
10. Prince, H. E. Biomarkers for diagnosing and monitoring autoimmune diseases. *Biomarkers* (2005). doi:10.1080/13547500500214194
11. Gubala, V., Harris, L. F., Ricco, A. J., Tan, M. X. & Williams, D. E. Point of care diagnostics: Status and future. *Analytical Chemistry* (2012). doi:10.1021/ac2030199
12. Löwik, D. W. P. M., Ayres, L., Smeenk, J. M. & Hest, J. C. M. Van. Synthesis of Bio-Inspired Hybrid Polymers Using Peptide Synthesis and Protein Engineering. *Adv. Polym. Sci.* (2006). doi:10.1007/12
13. Wang, Y., Ye, Z. & Ying, Y. New trends in impedimetric biosensors for the detection of foodborne pathogenic bacteria. *Sensors* (2012). doi:10.3390/s120303449
14. Berger, A. H. & Bhown, A. S. Comparing physisorption and chemisorption solid sorbents for use separating CO2 from flue gas using temperature swing adsorption. in *Energy Procedia* (2011). doi:10.1016/j.egypro.2011.01.089

15. Briand, E. *et al.* Building of an immunosensor: How can the composition and structure of the thiol attachment layer affect the immunosensor efficiency? *Biosens. Bioelectron.* (2006). doi:10.1016/j.bios.2006.05.018

16. Swierczewska, M., Liu, G., Lee, S. & Chen, X. High-sensitivity nanosensors for biomarker detection. *Chemical Society Reviews* (2012). doi:10.1039/c1cs15238f

17. Homola, J. Present and future of surface plasmon resonance biosensors. *Analytical and Bioanalytical Chemistry* (2003). doi:10.1007/s00216-003-2101-0

18. Goldberg, A. L. Protein degradation and protection against misfolded or damaged proteins. *Nature* (2003). doi:10.1038/nature02263

19. Sapsford, K. E., Pons, T., Medintz, I. L. & Mattoussi, H. Biosensing with luminescent semiconductor quantum dots. *Sensors* (2006). doi:10.3390/s6080925

20. Vo-Dinh, T. & Cullum, B. Biosensors and biochips: Advances in biological and medical diagnostics. *Fresenius' Journal of Analytical Chemistry* (2000). doi:10.1007/s002160051549

21. Braden, B. C. *et al.* Protein motion and lock and key complementarity in antigen-antibody reactions. *Pharm. Acta Helv.* (1995). doi:10.1016/0031-6865(94)00046-X

22. Marazuela, M. D. & Moreno-Bondi, M. C. Fiber-optic biosensors - An overview. *Analytical and Bioanalytical Chemistry* (2002). doi:10.1007/s00216-002-1235-9

23. Teles, F. R. R. & Fonseca, L. P. Trends in DNA biosensors. *Talanta* **77,** 606–623 (2008).

24. Lagarde, F. & Jaffrezic-Renault, N. Cell-based electrochemical biosensors for water quality assessment. *Analytical and Bioanalytical Chemistry* (2011). doi:10.1007/s00216-011-4816-7

25. Sassolas, A., Leca-Bouvier, B. D. & Blum, L. J. DNA biosensors and microarrays. *Chemical Reviews* **108,** 109–139 (2008).

26. Haes, A. J. & Van Duyne, R. P. A nanoscale optical biosensor: Sensitivity and selectivity of an approach based on the localized surface plasmon resonance spectroscopy of triangular silver nanoparticles. *J. Am. Chem. Soc.* (2002). doi:10.1021/ja020393x

27. Patterson, A. S., Hsieh, K., Soh, H. T. & Plaxco, K. W. Electrochemical real-time nucleic acid amplification: Towards point-of-care quantification of pathogens. *Trends in Biotechnology* (2013). doi:10.1016/j.tibtech.2013.09.005

28. Pensa, E. *et al.* The chemistry of the sulfur-gold interface: In search of a unified model. *Acc. Chem. Res.* (2012). doi:10.1021/ar200260p

29. Zhang, K., Ma, H., Zhang, L. & Zhang, Y. Fabrication of a sensitive impedance biosensor of DNA hybridization based on gold nanoparticles modified gold electrode. *Electroanalysis* (2008). doi:10.1002/elan.200804290

30. Nagasaki, Y. Construction of a densely poly(ethylene glycol)-chain-tethered surface and its performance. *Polymer Journal* (2011). doi:10.1038/pj.2011.93

31. Jinhao, G. A. O., Hongwei, G. U. & Bing, X. U. Multifunctional magnetic nanoparticles: design, synthesis, and biomedical applications. *Acc. Chem. Res.* (2009). doi:10.1021/ar9000026

32. Ngo, V. K. T. *et al.* Quartz crystal microbalance (QCM) as biosensor for the detecting of Escherichia coli O157:H7. *Adv. Nat. Sci. Nanosci. Nanotechnol.* (2014). doi:10.1088/2043-6262/5/4/045004

33. Pei, J., Tian, F. & Thundat, T. Glucose biosensor based on the microcantilever. *Anal Chem* (2004). doi:10.1021/ac035048k

34. Marinelli, M., Mercuri, F., Zammit, U. & Pizzoferrato, R. The influence of the coupling fluids and of the pyroelectric transducer on low-temperature photopyroelectric studies. *Appl. Phys. A Solids Surfaces* (1991). doi:10.1007/BF00323726

35. Xiao, Y. & Isaacs, S. N. Enzyme-Linked Immunosorbent Assay (ELISA) and Blocking with Bovine Serum Albumin (BSA) -Not all BSAs are alike. *J Immunol Methods* **384,** 148–151 (2012).

36. Mohammad, K. & Esen, A. A blocking agent and a blocking step are not needed in ELISA, immunostaining dot-blots and Western blots. *J. Immunol. Methods* **117,** 141–145 (1989).

37. Steinitz, M. Quantitation of the blocking effect of Tween 20 and bovine serum albumin in ELISA microwells. *Anal. Biochem.* **282,** 232–238 (2000).

38. Jeyachandran, Y. L., Mielczarski, J. A., Mielczarski, E. & Rai, B. Efficiency of blocking of non-specific interaction of different proteins by BSA adsorbed on hydrophobic and hydrophilic surfaces. *J. Colloid Interface Sci.* **341,** 136–142 (2010).

39. Vogt, R. V., Phillips, D. L., Omar Henderson, L., Whitfield, W. & Spierto, F. W. Quantitative differences among various proteins as blocking agents for ELISA microtiter plates. *J. Immunol. Methods* (1987). doi:10.1016/0022-1759(87)90214-6

40. Konradi, R., Acikgoz, C. & Textor, M. Polyoxazolines for nonfouling surface coatings - A direct comparison to the gold standard PEG. *Macromolecular Rapid Communications* (2012). doi:10.1002/marc.201200422

41. VandeVondele, S., Vörös, J. & Hubbell, J. A. RGD-grafted poly-L-lysine-graft-(polyethylene glycol) copolymers block non-specific protein adsorption while promoting cell adhesion. *Biotechnol. Bioeng.* (2003). doi:10.1002/bit.10625

42. Thierry, B. *et al.* Electrostatic self-assembly of PEG copolymers onto porous silica nanoparticles. *Langmuir* (2008). doi:10.1021/la8007206

43. Guo, W. H. & Wang, Y. L. Micropatterning cell-substrate adhesions using linear polyacrylamide as the blocking agent. *Cold Spring Harb. Protoc.* **6,** (2011).

44. Liu, B., Huang, P. J. J., Kelly, E. Y. & Liu, J. Graphene oxide surface blocking agents can increase the DNA biosensor sensitivity. *Biotechnol. J.* **11,** 780–787 (2016).

45. Haycock, J. W. Polyvinylpyrrolidone as a Blocking Agent in Immunochemical Studies.

Anal. Biochem. **208,** 397–399 (1993).

46. Riquelme, M. V *et al.* Optimizing blocking of nonspecific bacterial attachment to impedimetric biosensors. *Sens. Bio-Sensing Res.* **8,** 47–54 (2016).

47. Liu, B. *et al.* Parts-per-million of polyethylene glycol as a non-interfering blocking agent for homogeneous biosensor development. *Anal. Chem.* **85,** 10045–10050 (2013).

48. Kim, P., Kreder, M. J., Alvarenga, J. & Aizenberg, J. Hierarchical or not? Effect of the length scale and hierarchy of the surface roughness on omniphobicity of lubricant-infused substrates. *Nano Lett.* (2013). doi:10.1021/nl4003969

49. Manna, U. & Lynn, D. M. Fabrication of liquid-infused surfaces using reactive polymer multilayers: Principles for manipulating the behaviors and mobilities of aqueous fluids on slippery liquid interfaces. *Adv. Mater.* (2015). doi:10.1002/adma.201500893

50. Ma, W., Higaki, Y., Otsuka, H. & Takahara, A. Perfluoropolyether-infused nano-texture: A versatile approach to omniphobic coatings with low hysteresis and high transparency. *Chem. Commun.* (2013). doi:10.1039/c2cc37576a

51. He, W., Liu, P., Zhang, J. & Yao, X. Emerging Applications of Bioinspired Slippery Surfaces in Biomedical Fields. *Chemistry - A European Journal* (2018). doi:10.1002/chem.201801368

52. Cao, M. *et al.* Water-Repellent Properties of Superhydrophobic and Lubricant-Infused 'slippery' Surfaces: A Brief Study on the Functions and Applications. *ACS Appl. Mater. Interfaces* (2016). doi:10.1021/acsami.5b07881

53. Bohn, H. F. & Federle, W. Insect aquaplaning: Nepenthes pitcher plants capture prey with the peristome, a fully wettable water-lubricated anisotropic surface. *Proc. Natl. Acad. Sci.* (2004). doi:10.1073/pnas.0405885101

54. Wong, T.-S. *et al.* Bioinspired self-repairing slippery surfaces with pressure-stable omniphobicity. *Nature* **477,** 443–7 (2011).

55. Anand, S., Paxson, A. T., Dhiman, R., Smith, J. D. & Varanasi, K. K. Enhanced Condensation on Lubricant- Impregnated Nanotextured Surfaces. *ACS Nano* (2012). doi:10.1021/nn303867y

56. Smith, J. D. *et al.* Droplet mobility on lubricant-impregnated surfaces. *Soft Matter* (2013). doi:10.1039/c2sm27032c

57. Daniel, D., Mankin, M. N., Belisle, R. A., Wong, T. S. & Aizenberg, J. Lubricant-infused micro/nano-structured surfaces with tunable dynamic omniphobicity at high temperatures. *Appl. Phys. Lett.* **102,** (2013).

58. Yuan, S., Luan, S., Yan, S., Shi, H. & Yin, J. Facile Fabrication of Lubricant-Infused Wrinkling Surface for Preventing Thrombus Formation and Infection. *ACS Appl. Mater. Interfaces* (2015). doi:10.1021/acsami.5b05865

59. Roy, P. K., Pant, R., Nagarajan, A. K. & Khare, K. Mechanically Tunable Slippery Behavior on Soft Poly(dimethylsiloxane)-Based Anisotropic Wrinkles Infused with

Lubricating Fluid. *Langmuir* (2016). doi:10.1021/acs.langmuir.6b00865

60. Kamei, J. & Yabu, H. On-Demand Liquid Transportation Using Bioinspired Omniphobic Lubricated Surfaces Based on Self-Organized Honeycomb and Pincushion Films. *Adv. Funct. Mater.* **25,** 4195–4201 (2015).

61. Badv, M., Jaffer, I. H., Weitz, J. I. & Didar, T. F. An omniphobic lubricant-infused coating produced by chemical vapor deposition of hydrophobic organosilanes attenuates clotting on catheter surfaces. *Sci. Rep.* **7,** (2017).

62. Kim, P. *et al.* Liquid-infused nanostructured surfaces with extreme anti-ice and anti-frost performance. *ACS Nano* (2012). doi:10.1021/nn302310q

63. Wilson, P. W. *et al.* Inhibition of ice nucleation by slippery liquid-infused porous surfaces (SLIPS). *Phys. Chem. Chem. Phys.* (2013). doi:10.1039/c2cp43586a

64. Xiao, L. *et al.* Slippery liquid-infused porous surfaces showing marine antibiofouling properties. *ACS Appl. Mater. Interfaces* (2013). doi:10.1021/am402635p

65. You, I., Lee, T. G., Nam, Y. S. & Lee, H. Fabrication of a micro-omnifluidic device by omniphilic/omniphobic patterning on nanostructured surfaces. *ACS Nano* (2014). doi:10.1021/nn502226v

66. Leslie, D. C. *et al.* A bioinspired omniphobic surface coating on medical devices prevents thrombosis and biofouling. *Nat. Biotechnol.* (2014). doi:10.1038/nbt.3020

67. Appeltans, W. *et al.* The magnitude of global marine species diversity. *Curr. Biol.* (2012). doi:10.1016/j.cub.2012.09.036

68. Franklin, P. A. Dissolved oxygen criteria for freshwater fish in New Zealand: A revised approach. *New Zealand Journal of Marine and Freshwater Research* (2014). doi:10.1080/00288330.2013.827123

69. Sánchez, E. *et al.* Use of the water quality index and dissolved oxygen deficit as simple indicators of watersheds pollution. *Ecol. Indic.* (2007). doi:10.1016/j.ecolind.2006.02.005

70. Fletcher, M. & Loeb, G. I. Influence of substratum characteristics on the attachment of a marine pseudomonad to solid surfaces. *Appl. Environ. Microbiol.* (1979).

71. O'Toole, G., Kaplan, H. B. & Kolter, R. Biofilm Formation as Microbial Development. *Annu. Rev. Microbiol.* (2000). doi:10.1146/annurev.micro.54.1.49

72. Maunders, E. & Welch, M. Matrix exopolysaccharides; the sticky side of biofilm formation. *FEMS Microbiology Letters* (2017). doi:10.1093/femsle/fnx120

73. Kregiel, D. Advances in biofilm control for food and beverage industry using organo-silane technology: A review. *Food Control* (2014). doi:10.1016/j.foodcont.2013.11.014

74. Sano, K. *et al.* The development of the anti-biofouling coating agent using metal nanoparticles and analysis by Raman spectroscopy and FIB system. *Surf. Coatings Technol.* (2017). doi:10.1016/j.surfcoat.2017.04.015

75. Zhu, X., Bai, R., Wee, K. H., Liu, C. & Tang, S. L. Membrane surfaces immobilized with

ionic or reduced silver and their anti-biofouling performances. *J. Memb. Sci.* (2010). doi:10.1016/j.memsci.2010.07.041

76. Shanmugasundaram, T., Radhakrishnan, M., Gopikrishnan, V., Pazhanimurugan, R. & Balagurunathan, R. A study of the bactericidal, anti-biofouling, cytotoxic and antioxidant properties of actinobacterially synthesised silver nanoparticles. *Colloids Surfaces B Biointerfaces* (2013). doi:10.1016/j.colsurfb.2013.06.045

77. Carl, C. *et al.* Enhancing the efficacy of fouling-release coatings against fouling by Mytilus galloprovincialis using nanofillers. *Biofouling* (2012). doi:10.1080/08927014.2012.728588

78. Van Houdt, R. & Michiels, C. W. Biofilm formation and the food industry, a focus on the bacterial outer surface. *Journal of Applied Microbiology* (2010). doi:10.1111/j.1365-2672.2010.04756.x

79. Buxadera-Palomero, J. *et al.* Antifouling coatings for dental implants: Polyethylene glycol-like coatings on titanium by plasma polymerization. *Biointerphases* (2015). doi:10.1116/1.4913376

80. Wisniewski, N. & Reichert, M. Methods for reducing biosensor membrane biofouling. *Colloids and Surfaces B: Biointerfaces* (2000). doi:10.1016/S0927-7765(99)00148-4

81. Ito, Y., Hasuda, H., Sakuragi, M. & Tsuzuki, S. Surface modification of plastic, glass and titanium by photoimmobilization of polyethylene glycol for antibiofouling. *Acta Biomater.* (2007). doi:10.1016/j.actbio.2007.05.010

82. Miller, D. J. *et al.* Short-term adhesion and long-term biofouling testing of polydopamine and poly(ethylene glycol) surface modifications of membranes and feed spacers for biofouling control. *Water Res.* (2012). doi:10.1016/j.watres.2012.03.058

83. Ware, C. S. *et al.* Marine Antifouling Behavior of Lubricant-Infused Nanowrinkled Polymeric Surfaces. *ACS Appl. Mater. Interfaces* (2018). doi:10.1021/acsami.7b14736

84. Wang, L. & McCarthy, T. J. Covalently Attached Liquids: Instant Omniphobic Surfaces with Unprecedented Repellency. *Angew. Chemie - Int. Ed.* (2016). doi:10.1002/anie.201509385

85. Leslie, D. C. *et al.* A bioinspired omniphobic surface coating on medical devices prevents thrombosis and biofouling. *Nat. Biotechnol.* **32,** 1134–1140 (2014).

86. Hsu, L. *et al.* Development of a low-cost hemin-based dissolved oxygen sensor with anti-biofouling coating for water monitoring. *IEEE Sens. J.* (2014). doi:10.1109/JSEN.2014.2332513

87. Wang, P., Zhang, D. & Lu, Z. Slippery liquid-infused porous surface bio-inspired by pitcher plant for marine anti-biofouling application. *Colloids Surfaces B Biointerfaces* (2015). doi:10.1016/j.colsurfb.2015.09.019

88. Tomaszewska, M., Gryta, M. & Morawski, A. W. Mass transfer of HCl and H2O across the hydrophobic membrane during membrane distillation. *J. Memb. Sci.* (2000). doi:10.1016/S0376-7388(99)00263-X

89. Zazouli, M. a, Ulbricht, M., Nasseri, S. & Susanto, H. Effect of hydrophilic and hydrophobic organic matter on amoxicillin and cephalexin residuals rejection from water by nanofiltration. *Iran. J. Environ. Heal. Sci. Eng.* (2010).

90. Chen, J. *et al.* An immobilized liquid interface prevents device associated bacterial infection in vivo. *Biomaterials* (2017). doi:10.1016/j.biomaterials.2016.09.028

91. Kratochvil, M. J. *et al.* Slippery Liquid-Infused Porous Surfaces that Prevent Bacterial Surface Fouling and Inhibit Virulence Phenotypes in Surrounding Planktonic Cells. *ACS Infect. Dis.* (2016). doi:10.1021/acsinfecdis.6b00065

92. Wang, P., Zhang, D., Sun, S., Li, T. & Sun, Y. Fabrication of slippery lubricant-infused porous surface with high underwater transparency for the control of marine biofouling. *ACS Appl. Mater. Interfaces* (2017). doi:10.1021/acsami.6b09117

93. Epstein, A. K., Wong, T.-S., Belisle, R. A., Boggs, E. M. & Aizenberg, J. Liquid-infused structured surfaces with exceptional anti-biofouling performance. *Proc. Natl. Acad. Sci.* (2012). doi:10.1073/pnas.1201973109

94. Liu, Z.-Z., Wang, Q., Liu, X. & Bao, J.-Q. Effects of amino-terminated self-assembled monolayers on nucleation and growth of chemical vapor-deposited copper films. *Thin Solid Films* **517,** 635–640 (2008).

95. Tsai, W. T. Environmental property modeling of perfluorodecalin and its implications for environmental fate and hazards. *Aerosol Air Qual. Res.* (2011). doi:10.4209/aaqr.2010.12.0106

96. Pittman, R. N. Regulation of Tissue Oxygenation. *Colloq. Ser. Integr. Syst. Physiol. From Mol. to Funct.* (2011). doi:10.4199/C00029ED1V01Y201103ISP017

97. Leslie, D. C. *et al.* A bioinspired omniphobic surface coating on medical devices prevents thrombosis and biofouling. *Nat. Biotechnol.* **32,** 1134 (2014).

98. Ilkhani, H., Hughes, T., Li, J., Zhong, C. J. & Hepel, M. Nanostructured SERS-electrochemical biosensors for testing of anticancer drug interactions with DNA. *Biosens. Bioelectron.* (2016). doi:10.1016/j.bios.2016.01.068

99. Gao, Q., Zhang, W., Guo, Y., Qi, H. & Zhang, C. Highly sensitive impedimetric sensing of DNA hybridization based on the target DNA-induced displacement of gold nanoparticles attached to ssDNA probe. *Electrochem. commun.* (2011). doi:10.1016/j.elecom.2011.01.018

100. Sun, L., Hu, N., Peng, J., Chen, L. & Weng, J. Ultrasensitive detection of mitochondrial DNA mutation by graphene oxide/DNA hydrogel electrode. *Adv. Funct. Mater.* (2014). doi:10.1002/adfm.201402191

101. Schena, M. *et al.* Microarrays: Biotechnology's discovery platform for functional genomics. *Trends in Biotechnology* (1998). doi:10.1016/S0167-7799(98)01219-0

102. Han, F., Huynh, B. H., Ma, Y. & Lin, B. High-efficiency DNA separation by capillary electrophoresis in a polymer solution with ultralow viscosity. *Anal. Chem.* (1999). doi:10.1021/ac990160x

103. Frankfurt, O. S. & Krishan, A. Identification of apoptotic cells by formamide-induced DNA denaturation in condensed chromatin. *J. Histochem. Cytochem.* (2001). doi:10.1177/002215540104900311

104. Bartels, C. L. & Tsongalis, G. J. MicroRNAs: Novel Biomarkers for Human Cancer. *Clin. Chem.* (2009). doi:10.1373/clinchem.2008.112805

105. Strehlitz, B., Nikolaus, N. & Stoltenburg, R. Protein detection with aptamer biosensors. *Sensors* (2008). doi:10.3390/s8074296

106. Liao, J. C. *et al.* Development of an advanced electrochemical DNA biosensor for bacterial pathogen detection. *J. Mol. Diagn.* (2007). doi:10.2353/jmoldx.2007.060052

107. Ivnitski, D., Abdel-Hamid, I., Atanasov, P. & Wilkins, E. Biosensors for detection of pathogenic bacteria. *Biosensors and Bioelectronics* (1999). doi:10.1016/S0956-5663(99)00039-1

108. Wang, J. *et al.* DNA electrochemical biosensor for the detection of short DNA sequences related to the human immunodeficiency virus. *Anal. Chem.* (1996). doi:10.1021/ac9602433

109. Deng, J. & Toh, C. S. Impedimetric DNA biosensor based on a nanoporous alumina membrane for the detection of the specific oligonucleotide sequence of dengue virus. *Sensors (Switzerland)* (2013). doi:10.3390/s130607774

110. Benvidi, A. *et al.* A highly sensitive and selective electrochemical DNA biosensor to diagnose breast cancer. *J. Electroanal. Chem.* (2015). doi:10.1016/j.jelechem.2015.05.002

111. Soper, S. A. *et al.* Point-of-care biosensor systems for cancer diagnostics/prognostics. in *Biosensors and Bioelectronics* (2006). doi:10.1016/j.bios.2006.01.006

112. Wang, J. Electrochemical biosensors: Towards point-of-care cancer diagnostics. in *Biosensors and Bioelectronics* (2006). doi:10.1016/j.bios.2005.10.027

113. Bagwe, R. P., Hilliard, L. R. & Tan, W. Surface modification of silica nanoparticles to reduce aggregation and nonspecific binding. *Langmuir* (2006). doi:10.1021/la052797j

114. Berg, C., Schindler, T., Niedner-Schatteburg, G. & Bondybey, V. E. Reactions of simple hydrocarbons with Nbn+: Chemisorption and physisorption on ionized niobium clusters. *J. Chem. Phys.* (1995). doi:10.1063/1.469535

115. Johnson, D. A., Gautsch, J. W., Sportsman, J. R. & Elder, J. H. Improved technique utilizing nonfat dry milk for analysis of proteins and nucleic acids transferred to nitrocellulose. *Gene Anal. Tech.* (1984). doi:10.1016/0735-0651(84)90049-9

116. Bergstrand, A., Rahmani-Monfared, G., Östlund, Å., Nydén, M. & Holmberg, K. Comparison of PEI-PEG and PLL-PEG copolymer coatings on the prevention of protein fouling. *J. Biomed. Mater. Res. - Part A* **88,** 608–615 (2009).

117. Winblade, N. D., Nikolic, I. D., Hoffman, a S. & Hubbell, J. a. Blocking adhesion to cell and tissue surfaces by the chemisorption of a poly-L-lysine-graft-(poly(ethylene glycol); phenylboronic acid) copolymer. *Biomacromolecules* (2000). doi:10.1021/bm000040v

118. Yang, J., Song, H., Ji, H. & Chen, B. Slippery lubricant-infused textured aluminum surfaces. *J. Adhes. Sci. Technol.* (2014). doi:10.1080/01694243.2014.933563

119. Tuteja, A., Choi, W., Mabry, J. M., McKinley, G. H. & Cohen, R. E. Robust omniphobic surfaces. *Proc. Natl. Acad. Sci.* (2008). doi:10.1073/pnas.0804872105

120. Schellenberger, F. *et al.* Direct observation of drops on slippery lubricant-infused surfaces. *Soft Matter* (2015). doi:10.1039/c5sm01809a

121. Zhang, F. *et al.* Chemical vapor deposition of three aminosilanes on silicon dioxide: Surface characterization, stability, effects of silane concentration, and cyanine dye adsorption. *Langmuir* **26,** 14648–14654 (2010).

122. Sotiri, I., Overton, J. C., Waterhouse, A. & Howell, C. Immobilized liquid layers: A new approach to anti-adhesion surfaces for medical applications. *Exp. Biol. Med.* (2016). doi:10.1177/1535370216640942

123. Yuan, S. *et al.* Liquid-Infused Poly(styrene-b-isobutylene-b-styrene) Microfiber Coating Prevents Bacterial Attachment and Thrombosis. *ACS Appl. Mater. Interfaces* (2016). doi:10.1021/acsami.6b06407

124. Manabe, K., Kyung, K. H. & Shiratori, S. Biocompatible slippery fluid-infused films composed of chitosan and alginate via layer-by-layer self-assembly and their antithrombogenicity. *ACS Appl. Mater. Interfaces* (2015). doi:10.1021/am508393n

125. Schousboe, I. β2-Glycoprotein I: A Plasma Inhibitor of the Contact Activation of the Intrinsic Blood Coagulation Pathway. *Blood* (1985).

126. Wu, Y. Contact pathway of coagulation and inflammation. *Thrombosis Journal* (2015). doi:10.1186/s12959-015-0048-y

127. Linke, B., Kiwit, M., Thomas, K., Krahwinkel, M. & Kerner, W. Prevention of the decrease in sensitivity of an amperometric glucose sensor in undiluted human serum. *Clin. Chem.* (1999).

128. Bonanno, L. M. & DeLouise, L. A. Whole blood optical biosensor. *Biosens. Bioelectron.* (2007). doi:10.1016/j.bios.2007.05.008

129. Christiaens, P. *et al.* EDC-mediated DNA attachment to nanocrystalline CVD diamond films. *Biosens. Bioelectron.* (2006). doi:10.1016/j.bios.2005.12.013

130. Bhattacharya, S., Datta, A., Berg, J. M. & Gangopadhyay, S. Studies on surface wettability of poly(dimethyl) siloxane (PDMS) and glass under oxygen-plasma treatment and correlation with bond strength. *J. Microelectromechanical Syst.* (2005). doi:10.1109/JMEMS.2005.844746

131. Siow, K. S., Britcher, L., Kumar, S. & Griesser, H. J. Plasma methods for the generation of chemically reactive surfaces for biomolecule immobilization and cell colonization - A review. *Plasma Processes and Polymers* **3,** 392–418 (2006).

132. Nakano, S. I., Karimata, H., Ohmichi, T., Kawakami, J. & Sugimoto, N. The effect of molecular crowding with nucleotide length and cosolute structure on DNA duplex

stability. *J. Am. Chem. Soc.* (2004). doi:10.1021/ja0463029

133. Shangguan, D. *et al.* Cell-specific aptamer probes for membrane protein elucidation in cancer cells. *J. Proteome Res.* (2008). doi:10.1021/pr700894d

134. Ali, M. M., Aguirre, S. D., Lazim, H. & Li, Y. Fluorogenic DNAzyme probes as bacterial indicators. *Angew. Chemie - Int. Ed.* (2011). doi:10.1002/anie.201100477

135. Barbulovic-Nad, I., Yang, H., Park, P. S. & Wheeler, A. R. Digital microfluidics for cell-based assays. *Lab Chip* (2008). doi:10.1039/b717759c

136. Hosseini, A. *et al.* Conductive Electrochemically Active Lubricant-Infused Nanostructured Surfaces Attenuate Coagulation and Enable Friction-Less Droplet Manipulation. *Advanced Materials Interfaces* (2018). doi:10.1002/admi.201800617